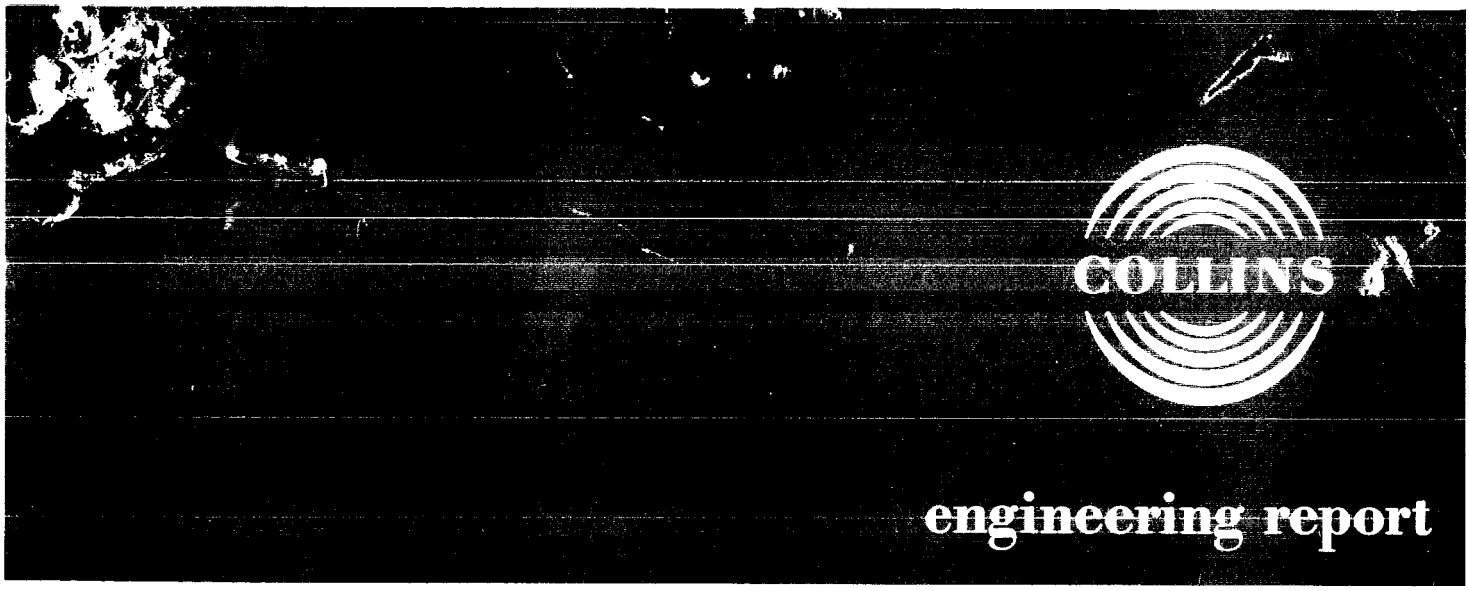

engineering report

Dallas Division | Collins Radio Company, Dallas, Texas

Copy no. 2

523-0556301-001D3M
17 April 1964

COLLINS

engineering report

GSFC Four Stations Rosman I System Test Final Report

Prepared by
R.T. Hart
Space Systems Division
Dallas Division, Collins Radio Company

Prepared for
Goddard Space Flight Center
Contract NAS5-2462

Dallas Division | Collins Radio Company, Dallas, Texas
Printed in U. S. A.

table of contents

list of tables

list of illustrations

list of illustrations (cont)

section 1

introduction

1.1 GENERAL.

The NASA Scientific Space Program has been enhanced with the installation of a Satellite Tracking Facility at Rosman, North Carolina. This facility is designed around an 85-foot-diameter parabolic antenna constructed on an X-Y mount.

This is the first of a series of similar installations to be made at strategic locations throughout the world. This network was primarily designed as a ground-based installation for the advanced weather satellite series. However, the broad design capabilities allow its usage to extend to all the scientific space programs.

Collins Radio Company is proud to participate in this venture. This report concerns the performance of Collins-supplied equipment for the Rosman station as well as the overall system performance related to tracking capability.

The site location chosen has proven ideal. The natural shielding has eliminated interfering signals that would normally degrade system performance. Climatic conditions for the area are relatively mild, eliminating the need for special environmental equipment.

The Rosman station participated in NASA tracking activities for the initial orbit of the IMP satellite. Both telemetry and tracking data were supplied by the station to complement the data supplied by other NASA stations.

Station installation and checkout was completed in early December 1963.

1.2 REVIEW OF COLLINS CONTRIBUTION.

While no single company has acted as prime contractor, the Space Systems Division of Collins Radio Company has worked closely with NASA to provide systems

engineering for the Rosman tracking facility. With the exception of the antenna structure, the same group installed the tracking equipment, including the antenna feed assembly, the tracking and telemetry receivers, a satellite command transmitter and antenna, and designed, built, and installed the servosystem.

Companies furnishing equipment on a subcontract include:

COMPANY	EQUIPMENT FURNISHED
Rantec	Antenna Feeds
ITT	Tracking Receivers
DEI	Telemetry Receivers
Vickers	Hydraulic Servo Components
ISC	Data Handling Equipment
AIL	Parametric Amplifiers
Hewlett-Packard	Test Equipment

Upon completion of the installation phase, an extensive test program was implemented and the results of those tests are the basis of this report. The tests were conducted by Collins and supported by a government-furnished aircraft during portions of the dynamic test phase. Ephemeris data for both stars and satellites were supplied by NASA.

During the course of the Rosman I program, monthly interim development reports were published covering each of the subsystems. These reports are entitled "Progress Report for GSFC Four Stations," copy numbers IDR-D549-1 through IDR-D549-22. To complement this report, it is encouraged that each of these reports be examined.

section 2

introduction to tests and results

2.1 GENERAL.

This report is based on performance tests conducted on site and include both static and dynamic tests. The static tests primarily determine the functional capabilities of each subsystem as related to the overall tracking accuracy. The dynamic tests are designed to evaluate the full capability of the system.

An extensive program was implemented to investigate all factors that would influence the performance. The following tabulation of results includes errors that may be used to bias the tracking data derived from operational conditions. These errors are known and repeatable and, when applied as correction factors, will enable high accuracy data to be produced by the station.

In the interest of providing a report for both system performance analysis and for system calibration at the site, the data presented in this report is derived from a comprehensive test program and presented in a manner useful for both purposes. In the data presented, notation is made when the data applies only to test purposes on-site and does not apply to system performance for tracking missions. This primarily refers to measurements made using the collimation tower where ground reflections affect the accuracy of the measurement. Each section contains a brief description of the test used as a further assistance to maintenance and calibration of the system.

2.1.1 ANTENNA ALIGNMENT.

The following summary of antenna alignment errors should be compared with the error equations which show how each of these component errors are combined to constitute the total error. These error equations and their accompanying descriptive

tables are presented for both encoder to optical and for encoder to r-f systems. The optical to encoder equations and table are in section 2.2.2.2. The r-f to encoder equations and table are in section 2.3.6.

(1) Structure.

(a) X-Axis Tilt. The north end is 0.001° up and 0.001° east.

(b) X- to Y-Axis Orthogonality. The angle between the positive (north and east) ends of the axes is 89.993°.

(2) Encoder and Optics.

(a) X-encoder bias is 0.014° (encoder value is too large).

(b) Y-axis to optical axis orthogonality — The angle between the positive (east and outward) ends of the axes is 90.005°.

(c) Y-encoder to optical axis bias is -0.301° (encoder value is too small). This value slipped from -0.032° to -0.301° between 3 October 1963 and 20 November 1963.

(3) R-F to Encoder.

(a) X-encoder bias is 0.014° (encoder value is too large).

(b) Y-encoder axis to r-f axis orthogonality — the angles between the outward and east ends of the r-f and Y-axes are:

1. 90.025° (136 mc)

2. 90.037° (400 mc)

3. 90.012° (1700 mc).

(c) X acceleration error coefficient is -0.321° (this is a dynamic lag in X) $K_a = \frac{1}{0.321} = 3.11 \text{ deg/sec}^2$

(d) Y-axis to r-f axis bias is:

1. -0.259° (136 mc)

2. -0.301° (400 mc)

3. -0.295° (1700 mc).

(In all cases, the encoder value is too small.)

(e) Y acceleration error coefficient is -0.135°. (This is a dynamic lag in Y) $K_a = \frac{1}{0.135} = 7.3 \text{ deg/sec}^2$.

2.1.2 TRACKING ACCURACY.

The tracking accuracy with known errors removed is as shown below:

(1) X rms:

(a) 0.032° (136 mc)

(b) 0.027° (400 mc)

(c) 0.003° (1700 mc)

(2) Y rms:

(a) 0.014° (136 mc)

(b) 0.021° (400 mc)

(c) 0.007° (1700 mc).

2.2 STATIC TESTS.

The static tests are defined as tests performed on stationary targets. These tests are included in four main categories:

(1) Pointing capability of the optical encoder system

(2) Tracking receiver performance

(3) Servo performance

(4) Tracking loop performance.

These tests cover parameters that might be expected from operational conditions. The test results describe the effects of each parameter and allow a comprehensive prediction of system performance to be made for a given operational mission.

2.2.1 OPTICAL BORESIGHT.

2.2.1.1 PURPOSE OF TEST. The purpose of this test is to determine the angle readout coordinates of the optical target and to determine repeatability of the encoder system. This is a direct measure of the system backlash.

To perform this test, the antenna is initially moved until the camera reticle and the optical target on the collimation tower are coincident. The antenna is then slewed away from the target and then returned in a manner to prevent overshoot. Each time

the optical system is correctly aligned and the encoder readings are recorded. The difference in successive encoder readings is a measure of the backlash.

2. 2. 1. 2 TEST ANALYSIS. The data presented in figure 2-1 indicates that the backlash in the Y system is 0. 0094°, while that in X is 0. 004°. The data also indicates that a deflection of 0. 004° in X resulted from the movement in Y although the X brakes were locked. With the Y brakes locked, a deflection of 0. 002° in Y was caused by the movement of the X axis.

The test was divided into four sections. The Y-axis was fixed in tests 1 and 2. The X-axis was then moved up and returned to an optical target, then moved down and returned to an optical target. Similar measurements were made in tests 3 and 4 with the X-axis held constant.

In a previously published report entitled "Determination of Errors in Antenna Shaft Position Measurement System at Rosman I Facility," CER-D1706, a similar measurement was made. The reader is encouraged to examine that report for additional information concerning the encoding system. The values determined from this test are also in close agreement with information determined from star shot data.

From tests 1 and 2, an average X value was determined and a Y value determined from tests 3 and 4. These values are recorded on figure 2-1 as X = 84. 225 and Y = -14. 883. These values are used throughout this report as the optical boresight coordinate of the collimation tower target. These values were determined from tests performed during the month of October. In the following sections of this report, tests indicate a shift in encoder alignment from the original values. Therefore, the true optical boresight may be different than that determined. This does not effect the backlash measurements.

2. 2. 2 STAR SHOTS.

2. 2. 2. 1 PURPOSE OF TEST. The purpose of this test is to determine the calibration of the angle encoder system to the optical system. This allows several alignment parameters to be determined, and is accomplished with two computer programs. The first solves for difference in X and Y angles between the measured and known values.

The second solves for 11 values of antenna alignment parameters that allow optical-to-encoder calibration, and the X and Y rms of the fit. This test is performed by positioning the antenna to optical stars over a broad coverage of pointing directions. The picture records time, star displacement from film center, X and Y encoder values at the recorded time, and a title block that gives the test and date.

2.2.2.2 TEST ANALYSIS. The results in table 2-1 show these alignment values and their definitions. This is based on three sets of star shot data comprising a total of 304 individual star shots. The three sets of data are from three separate nights over a period of 48 days. This allows system changes as well as system accuracy to be determined. Data from the last two dates is also combined as a weighted average. This average represents the final condition of the antenna, after changes as described below. Probable errors are given to show how accurately the parameters were determined. All units are in degrees of error.

The predicted errors between the optical and encoder systems are thus given by:

$$X(S)_E = S1 + S2 \sin (X-S3) + S4 \tan Y \sin X - S5 \tan Y \cos X + S6 \tan Y + S7/\cos Y$$

$$Y(S)_E = S8 + S9 \sin (Y-S10) + S4 \cos X + S5 \sin X \pm S11$$

where:

$X(S)_E$ and $Y(S)_E$ = the optical-to-encoder errors in X and Y.

These equations are also the normal equations that are used by the second (regression) program to provide a least squares solution of S1 through S11 and the X and Y rms of the residuals remaining after the fit. For a detailed description of the regression program, see appendix A of "Progress Report for GSFC Four Stations, 1 June to 30 June 1963." The "Zone 1" is given by the normal equations above. The first (star shot) program is described in appendix A of "Progress Report for GSFC Four Stations, 1 February to 28 February 1963." Note that the three antenna alignment parameters (S4, S5, and S6) are solved for in the regression program, rather than measured and then removed by the star shot program.

SYMBOL	DESCRIPTION	DATE / NO. OF STARS	10/3/63 49	11/18/63 91	11/20/63 164	AVERAGE 255
S1	X encoder bias		.002±.009	.021±.004	.011±.002	.014±.001
*S2	X deflection coefficient		-.013	-.021	-.024	-.024
*S3	X deflection offset		-17.197	-4.853	-14.323	-12.265
S4	Tilt component of the north end of the X axis in an upward direction (a negative sign means tilt is down)		-.005±.003	.000±.002	.001±.001	.001±.000
S5	Tilt component of the north end of the X axis in an eastward direction (a negative sign means tilt is westward)		.000±.001	.000±.001	.002±.001	.001±.001
*S6	X axis to Y axis lack of orthogonality (a negative sign means | S6| is added to 90°)		.003±.002	.008±.001	.007±.001	.007±.000
*S7	Optical axis to Y axis lack of orthogonality (a negative sign means | S7| is added to 90°)		.004±.007	-.012±.003	-.002±.002	-.005±.002
S8	Optical axis to Y encoder axis bias		-.032±.003	-.301±.002	-.301±.002	-.301±.000
*S9	Y deflection coefficient		.203	.219	.223	.222
*S10	Y deflection offset		-3.194	-2.119	-2.883	-2.579
*S11	Y hysteresis		.002±.001	-.001±.001	-.002±.001	-.001±.000
X(S)rms	X rms of the fit to the measured minus predicted values		.004	.008	.006	.007
Y(S)rms	Y rms of the fit to the measured minus predicted values		.006	.005	.005	.005

*The deflection terms and hysteresis require additional explanation. The deflection errors are solved using the form K sin (X-O) where O is the offset, or the point about which the deflection is symmetrical. K is just a coefficient, so the deflection error ranges roughly between +K and -K degrees as X (or Y) goes from +90 to -90 degrees. The Y hysteresis error is encountered whenever the Y encoder reverses direction and the error has the opposite sign to the direction of motion change, e.g., if Y is moving in a positive direction and then starts back in a negative direction, the direction change is negative, but the Y hysteresis error is positive. X hysteresis was found to be insignificant. Orthogonality terms reference the positive (north for X, east for Y, and outwardly directed for r-f) axes in all cases.

For these reasons, the system is sufficiently accurate for its intended purposes. If the station is to be used for orbital determination for future satellites, each parameter should be carefully considered.

2.2.3 RECEIVER ANALOG ERROR SIGNALS.

2.2.3.1 PURPOSE OF TEST. The purpose of this test is to measure the tracking error voltage produced by the tracking receiver as a function of target angular error and to determine its variation with respect to variation of the signal conditions.

To perform this test, a signal simulating a satellite is radiated from the collimation tower. The antenna is displaced from the target and a recording of the error as a function of the displacement is made. This measurement is repeated for each parameter change.

2.2.3.2 TEST ANALYSIS. The results of this test indicate that only a small variation may be expected in the error signals under all operational conditions. The servo system will readily accept a range of 6 db without serious degradation in performance. The maximum variation indicated by the test data presented in figures 2-2 through 2-5 is 3 db.

Minor variations between the three receivers are indicated in all tests. These are due to the agc circuits and the bandwidth filters. Essentially, no changes in the receiver analogs are experienced as a function of antenna polarization. Signal level and modulation produce minor effects in the amplitude of the analogs.

A nominal satellite track would use the following system parameters:

PARAMETERS	VALUES	ANALOG LEVEL BELOW MAXIMUM
AGC Time Constant	300 mc	-0.75 db
Bandwidth	100 cps	-1.85 db
Modulation	Pulse	-0.25 db
Polarization	RHC	-0.1 db
Receiver Frequency Most Used	136 mc	0
Nominal Signal Level	-125 dbm	-0.2 db

The data presented was derived from the figures of this section. From these results, a nominal satellite track on 136 mc would cause the system loop gain to be only -1.85 db below the maximum loop gain obtained from all conditions tested on the collimation tower (see figure 2-3).

Figures 2-6 through 2-10 are presented as typical analogs obtained by causing the antenna to slew past the collimation tower. These tests indicate the symmetry of the analogs about the zero amplitude point and the sidelobe characteristics outside the tracking beamwidth of the antenna. The relative amplitude scales are presented on the figures only for the purpose of comparing symmetry about the zero point.

The data presented in this section does not include the effects of pulse or frequency modulation. These two parameters were checked during the tracking stability test and showed no noticeable effect. Several of the satellites tracked during the test program used a form of pulse modulation that caused no degradation of system performance. From figure 2-2, it may be seen that an amplitude-modulated signal causes a slightly lower output than a CW signal for a receiver bandwidth of 100 cps. This is caused by a reduction in carrier level due to modulation, since the modulation sidebands are outside the receiver bandwidth. For this reason, pulse and FM would not change the performance of the system compared to CW signals if the average amplitudes of the signals are considered.

When signals are very near threshold, no agc action can take place in the receiver. This is true for signals similar to those received from radio stars and very weak satellites. With the subsequent loss in agc, the analog error signals may be excessively high and servo performance will be degraded. For this type of tracking mission, the servo gain should be reduced below the normal setting. The autotrack relay adjustment should be set to prevent the servo from tracking weak signals where the signal-to-noise ratio is poor.

2. 2. 4 STATIC ACQUISITION.

2. 2. 4. 1 PURPOSE OF TEST. The purpose of this test is to determine the servo system characteristics utilizing the antenna-receiver servoloop. From the previous test, a general analysis indicates a single loop gain setting is adequate for all signal conditions.

This test is performed by displacing the antenna from the collimation tower, and then allowing the antenna to acquire the target in an autotrack mode. The error signal is continuously recorded during this time.

2. 2. 4. 2 TEST ANALYSIS. The results of this test are presented in graphical form. Both axes were tested on each frequency. The data presented is typical of a broad range of parameters chosen. Changes in modulation, signal strength, polarization, and receiver bandwidth caused no apparent changes in performance. The damping effect noted on each test indicates proper loop gain and phase characteristics.

The data presented in figure 2-17 indicates antenna characteristics when both axes are allowed to acquire the target simultaneously. A slight reduction in gain in the X-axis would decrease the elliptical action indicated. The phasing of the feed assembly is such that no system instability is apparent due to crosstalk.

For all snap-on tests on the X-axis, an apparent effect is noted between the movement from below and from above. These tests are performed using the collimation tower where the X-angle is approximately 84°. This effect is caused by an unbalance in the structure. Proper amounts of counterbalance would cause these tests to be symmetrical. For this test, the Y-axis is moving in a horizontal plane where an imbalance, if present, would not be apparent.

2. 2. 5 ACQUISITION FROM INITIAL VELOCITY.

2. 2. 5. 1 PURPOSE OF TEST. The purpose of the constant velocity test is to determine the acquisition characteristics of the tracking system as a function of the relative velocity between the antenna and the target. To perform this test, a signal is radiated from the collimation tower and the antenna is displaced several beamwidths. The antenna is then caused to move at the desired velocity toward the target until it approaches the acquisition cone. When the antenna enters the acquisition cone, it is allowed to autotrack the target.

Data derived from a typical test is presented in figure 2-18. These tests indicate little change in performance due to an initial velocity.

2. 2. 5. 2 TEST ANALYSIS. The information presented was derived from tests at 400 mc. Similar results were experienced on other frequencies. Similar tests were run by allowing an aircraft to fly into the antenna beamwidth with the antenna pointed in a fixed direction. Acquisition was then made by enabling the autotrack mode, at which time the antenna acquired the aircraft and continued to follow. No acquisition problems

were experienced with either the aircraft or any of the satellites tracked during the test program, on either 136 or 400 mc. When using the aircraft at 1700 mc, acquisition was made by transferring from either 136 or 400 mc to 1700 mc during a track. In all cases of the aircraft track, transfer from any frequency to either of the other two frequencies presented no problems.

2.2.6 R-F BORESIGHT.

2.2.6.1 PURPOSE OF TEST. The purpose of this test is to determine the relationship between the optical boresight and the r-f boresight. The optical boresight has been determined from a previous test. The r-f boresight is determined by allowing the system to autotrack a CW signal radiated from the collimation tower. For each polarization and frequency chosen, the antenna is allowed to acquire the target several times. This allows both the repeatability and the average position to be determined. As a further check, a comparison is also made between the optical and r-f axes during an aircraft track. (See paragraph 2.3.3.)

2.2.6.2 TEST ANALYSIS. Examination of the data presented in figure 2-19 is somewhat misleading. A large distribution in boresight is exhibited on 136 mc with changes in feed polarization. This is primarily due to ground reflections. While tracking both an aircraft and satellites, changes in feed polarization exhibited no noticeable shift in boresight. Therefore, this data is representative of measurements made on the collimation tower, but do not accurately represent the relationship between optical and r-f boresight when used on actual satellites.

Therefore, this data may be used for calibration and test, but is not directly related to the tracking missions.

2.2.7 BORESIGHT SHIFT WITH POLARIZATION.

2.2.7.1 PURPOSE OF TEST. The primary purpose of the collimation system is for test and calibration. Each time the system is allowed to autotrack the collimation system, similar repeatable results will indicate proper operation of the system. The most significant change that is readily apparent is the r-f boresight position. As seen from paragraph 2.2.6 (r-f boresight test), a change in signal parameters contributes only a small change in pointing angle. A more significant change, from the standpoint

of repeatability, is due to ground reflections. In turn, the ground reflections are dependent on the orientation of the collimating antenna. The boresight shift as a function of the collimation antenna position is presented in figures 2-20, 2-21, and 2-22.

2.2.7.2 TEST ANALYSIS. This data indicates the ground reflections are reduced as frequency is increased which, in turn, is a function of antenna beamwidth. These effects are not present at high angles such as those used during satellite tracks. For any test on the collimation tower, the position of the collimating antenna should be considered and its position recorded in conjunction with the X and Y encoder positions. This shift is not apparent from satellites at higher angles as, for instance, when the satellite is tumbling. Note that the shift is a function of the antenna beamwidth by comparing the response at 136 mc versus 1700 mc. To perform the test at 1700 mc, a target was chosen in the far field of the antenna to derive a true measurement.

2.2.8 STATIC TRACKING STABILITY.

2.2.8.1 PURPOSE OF TEST. The purpose of the tracking stability test is to determine the effective jitter of the tracking loop and derive from this data the relationship to the causes of instability. This test is conducted in two parts:

(1) The system is allowed to track the collimation target for 10 minutes for each change in signal condition. The signal conditions include changes in modulation, frequency, and receiver bandwidth.

(2) A continuous 24-hour stability test is performed where the only change in signal condition is the tracking frequency.

2.2.8.2 TEST ANALYSIS. The data from the first test is presented in figures 2-23 and 2-24. From this data it is difficult to determine relationships between the parameters chosen and their effects on tracking stability, primarily because these effects are small. At the lower frequencies, the antenna beamwidth is large and instabilities due to changes in modulation are obscured by noise. At the highest frequency (1700 mc) no significant effect on stability is contributed by modulation. A relationship is evident between the receiver bandwidth and stability. Receiver bandwidth is related to signal-to-noise ratios and an increase in receiver bandwidth produces an equivalent effect of reducing the transmitter power level. Signal level used is -120 dbm.

The data presented in figures 2-25 and 2-26, derived from the second test, also indicate a relationship between tracking stability and frequency. This test indicates no significant change in stability as a function of time. At 136 mc, the average tracking stability is 0.005°. This implies that the probability of a single measurement being within an accuracy of 0.005° is 63 percent. Therefore, when measurements are made using similar tests to those described in this section, several tests should be made and the average of these will produce dependable information. In the data presented, each point is the average jitter for the period of the test. For the first test, the period of the test is 10 minutes and is 1 hour for the other test.

It should be noted that the antenna beamwidth at 136 mc is approximately 12.5°. Therefore, the average jitter is:

$$\frac{0.005}{12.5} \times 100 = 0.04 \text{ percent of the beamwidth.}$$

At 1700 mc, the jitter is recorded as 1.7 percent of the beamwidth. This apparent contradiction may be explained when the actual jitter is compared to the resolution of the encoding system. The jitter at 1700 mc is 0.0012°; the encoder resolution is 0.001°. The measurements are being made at the threshold of the measuring equipment at 1700 mc. For this reason, the stability is probably better than the resolution of the encoders. In either case, the instability is so small compared to the antenna beamwidth, that no change in signal level could be measured; thus, it has no effect on telemetry reception.

In figures 2-27 and 2-28, the actual encoder positions are recorded as derived from the 24-hour test. During the test, each frequency was tracked for a period of 1 hour and repeated every third hour. Again, each point is the average for the period. The variation in position for each frequency indicates the range of variation in the effective boresight position over a 24-hour period. This variation is examined in figure 2-29 by correlating the encoder readings with the variation in ambient temperature during the 24-hour period. Since it exhibited the highest tracking stability, 1700 mc was chosen. There is insufficient data to determine an exact temperature coefficient, but there is a relationship that should be considered if high-accuracy pointing information is significant. The change in encoder readings is caused by

structural changes in the antenna. A time lag of approximately 3 hours is required for a positional change after a temperature change.

The approximate temperature coefficient is +0.0006°/°F for X and -0.0009°/°F for Y.

2.3 DYNAMIC TESTS.

The dynamic tests consist of those system tests that use a moving target. A variety of tests are performed to determine the system capability throughout the entire range of parameters expected in actual operation. To reduce the actual number of tests to be performed, selected parameters are used for the dynamic tests and comparisons are made to information derived from static tests.

Actual satellite tracks are used for test purposes, as well as an aircraft carrying suitable equipment to simulate satellite signals. By using an aircraft, the range of testing may be extended beyond the range of normal satellites to determine limiting cases. A sun track and a radio star track are also run to complement the other tests.

As a final check on the system, the program capability is determined. In this test, the true pointing angle versus predicted information recorded on program tape is determined.

Data from dynamic system tests allow two sets of system characteristics to be determined:

(1) The rms dynamic tracking accuracy in X and Y angles

(2) Instrument alignment parameters that relate dynamic tracking errors to specific terms such as bias, structural deflection, and antenna acceleration.

2.3.1 RADIO STAR TRACK.

The lowest antenna tracking rate performance is most easily determined from actually tracking a celestial object. In this test, the star Cassiopeia A is chosen. This star emits a broad range of electromagnetic radiation in the 136-mc region. It does not radiate visual light for optical tracking purposes. The geographic location of Rosman is such that Cassiopeia A may be tracked for approximately 20 hours of each 24-hour period. Both axes cover a broad range during the period.

The received signal level is low and is useful only on 136 mc for this test. To perform the test, wide bandwidth is used on the receiver. Otherwise, the conditions are similar to conventional satellite tracks. Parameters determined from this test compare favorably with information derived from the aircraft tracks of paragraph 2. 3. 3.

2. 3. 2 SUN TRACK.

This test is similar to the radio star track (paragraph 2. 3. 1) except the sun is tracked on a frequency of 1700 mc. Radio emission is too low from the star for use at 1700 mc and the sun provides too broad a source and is relatively weak for use on 136 mc. The use of both sources provides a comprehensive coverage of the full frequency range of the system.

Data reduction from this test also complemented the aircraft tracks as a verification of the accuracy of each of the parameters.

2. 3. 3 AIRCRAFT TRACKS.

2. 3. 3. 1 PURPOSE OF TEST. The purpose of aircraft tracks is to determine the calibration of the r-f system to the optical system for various system parameters under dynamic conditions. (See figure 2-30.)

An aircraft carrying equipment to simulate satellite signals was flown across the station under varying conditions of direction, altitude, velocity, and tracking frequency. The data consists of pictures of a target light on the aircraft, taken while the antenna tracked the aircraft. The pictures contain time, light displacement from the center of the film, X and Y encoder values at the recorded time, and a title block describing the test and date.

2. 3. 3. 2 TEST ANALYSIS. Two computer programs are used to solve for the r-f to optical calibration. The first makes two parallax corrections to the Y and X (actually cross Y) displacements of the aircraft from the film center, and computes encoder velocity and acceleration for the aircraft track. Parallax is caused by the camera offset from the center of the dish and the displacement of the light from the antenna on the aircraft. The second program solves for six values of antenna alignment parameters, which allow for r-f to optical calibration and the X and Y rms of the fit.

Aircraft tracks were run at three frequencies; 136, 400, and 1700 mc. To obtain a solution based on the largest possible distribution of input parameters, all runs from a given frequency were solved together. Table 2-2 first lists the r-f to optical boresights and tracking rms for each frequency, followed by weighted average values of deflection and acceleration coefficients over all three frequencies. During track, the servo system is type 2 and the steady-state velocity error is negligible. Probable errors indicate how accurately the parameters were determined. All units are in degrees of error, and the description of symbols is given in table 2-2.

The predicted errors between the r-f and optical systems are:

$$X(A)_E = A1 + A2 \sin X + A3\ddot{X} \cos Y$$

$$Y(A)_E = A5 + A6 \sin Y + A7\ddot{Y}$$

where:

$X(A)_E$ and $Y(A)_E$ = r-f to optical errors in X and Y

$\ddot{X}$ and $\ddot{Y}$ = X and Y acceleration

These equations are also the normal equations used by the second (regression) program to provide a least squares solution of A1 through A6 and the X and Y rms residuals remaining after the fit. Thus, all terms of the normal equations are known for the aircraft track data, except the A's, which the regression program solves for by inverting the matrix of coefficients. For a detailed description of the regression program, see appendix A of "Progress Report for GSFC Four Stations, 1 June to 30 June 1963." Note that "Zone 1" used the normal equations described above, and is based on film data rather than the prediction model shown in appendix A. The first program (aircraft track) is described in detail in appendix A of "Progress Report for GSFC Four Stations, 1 February to 28 February 1963." Parallax correction for the displacement on the aircraft of the r-f antenna to the light has now been added.

2.3.4 SATELLITE TRACKS.

A number of satellites were tracked during the test program to complement the other tests and to determine that, for the cases selected, the data derived from all other tests was in agreement. This correlation will determine that all dynamic conditions for any satellite track may be accurately predicted.

SYMBOL	DESCRIPTION	136 MC	400 MC	1700 MC
A1	X Boresight Between RF and Optical Axes	-.020 ±.001	-.032 ±.001	-.007 ±.001
A4	Y Boresight Between RF and Optical Axes	+.042 ±.001	+.000 ±.001	+.006 ±.001
X(A)rms	X Tracking RMS of the Fit to the Preceding Equations	+.032	+.027	+.003
Y(A)rms	Y Tracking RMS of the Fit to the Preceding Equations	+.014	+.021	+.007
		WEIGHTED AVERAGE OF THE THREE FREQUENCIES		
A2	X Deflection Coefficient	+.065 ±.005		
A3	X Acceleration Coefficient	-.321 ±.007		
A5	Y Deflection Coefficient	+.046 ±.005		
A6	Y Acceleration Coefficient	-.135 ±.017		

TABLE 2-2. TEST ANALYSIS

2. 3. 5 PROGRAMMED STAR TRACK.

2. 3. 5. 1 PURPOSE OF TEST. As a means of determining the capability of the program equipment to position the antenna along a precomputed path, the test is performed using stars to determine the accuracy. To perform this test, suitable stars are chosen and their predicted paths are punched on tape. The tape, in turn, is used to position the antenna while the camera photographs the star.

2. 3. 5. 2 TEST ANALYSIS. Data derived from the test is presented in figures 2-31 through 2-41. The relationship between predicted and actual values clearly indicates an offset in both axes. The offset is explainable due to the predicted values. The predictions were based on geographic coordinates other than the actual antenna location. The amount of error in X and Y due to incorrect coordinates is variable since it depends upon the position of the star being observed. A more significant portion of the offset is due to a possible shift in the encoders from the original alignment. See paragraph 2. 2. 2 (star shots). Neglecting offset, the test indicates that the antenna follows a program tape smoothly and with a high degree of accuracy over extended periods of time.

During the tests at Rosman, a similar offset was noticed during actual satellite tracks but in all cases the antenna was accurately positioned to the command position with respect to the encoders. All satellites tracked were readily acquired from the program mode, since the offset is only a small portion of the antenna beamwidth.

On each of the data sheets presented, the predicted ephemeris is recorded at a rate of one sample per minute, while the actual measured data is presented once for each 10 seconds. The response of the servo program loop may be observed from figures 2-32 and 2-34 where the actual film errors are recorded. Note that the deviation, or tracking jitter, is approximately $\pm 0.005°$ peak about the mean. This is negligible compared to the antenna beamwidth, even on the highest receiver frequencies. This is a true indication of the movement of the antenna reflector. It is a further indication of the servo system's capability to accurately position the antenna to a commanded position.

2.3.6 R-F TO ENCODER CALIBRATION.

The parameters that determine the r-f to encoder calibration may be obtained by adding the error equations from star shot tests and from aircraft track tests and combining similar terms. Since a different r-f to optical boresight exists for each of the three frequencies, these two terms will be referenced to a particular frequency. Note that these terms appear as part of the r-f to Y axis lack of orthogonality and as r-f axis to Y encoder axis bias in table 2-3.

The predicted errors between r-f and encoder systems are given by:

$$X(C)_E = C1 + [C2 \sin (X-C3) + C4 \sin X] + C5 \tan Y \sin X - C6 \tan Y \cos X + C7 \tan Y + \frac{C8}{\cos Y} + C9 \ddot{X}$$

$$Y(C)_E = C10 + [C11 \sin (X-C12) + C14 \sin X] + C5 \cos X + C6 \sin X + C13 \ddot{Y} \pm C15$$

where:

$X(C)_E$ and $Y(C)_E$ = R-f to encoder errors

$\ddot{X}$ and $\ddot{Y}$ = encoder accelerations in X and Y.

The sign convention for star shot and aircraft track tests is such that when the error equations of the two tests are added, a positive result means the encoder is reading a larger (more positive) value than the actual r-f direction. Thus, the true r-f position would be obtained by subtracting the positive error term from the measured encoder value. This sign convention applies term-by-term to the two r-f to encoder error equations. Note that a negative term means the true encoder reading would be obtained by increasing the measured encoder value by the amount of the error term.

2.3.6 R-F TO ENCODER CALIBRATION.

The parameters that determine the r-f to encoder calibration may be obtained by adding the error equations from star shot tests and from aircraft track tests and combining similar terms. Since a different r-f to optical boresight exists for each of the three frequencies, these two terms will be referenced to a particular frequency. Note that these terms appear as part of the r-f to Y axis lack of orthogonality and as r-f axis to Y encoder axis bias in table 2-3.

The predicted errors between r-f and encoder systems are given by:

$$X(C)_E = C1 + [C2 \sin (X-C3) + C4 \sin X] + C5 \tan Y \sin X - C6 \tan Y \cos X + C7 \tan Y + \frac{C8}{\cos Y} + C9 \ddot{X}$$

$$Y(C)_E = C10 + [C11 \sin (X-C12) + C14 \sin X] + C5 \cos X + C6 \sin X + C13 \ddot{Y} \pm C15$$

where:

$X(C)_E$ and $Y(C)_E$ = R-f to encoder errors

$\ddot{X}$ and $\ddot{Y}$ = encoder accelerations in X and Y.

The sign convention for star shot and aircraft track tests is such that when the error equations of the two tests are added, a positive result means the encoder is reading a larger (more positive) value than the actual r-f direction. Thus, the true r-f position would be obtained by subtracting the positive error term from the measured encoder value. This sign convention applies term-by-term to the two r-f to encoder error equations. Note that a negative term means the true encoder reading would be obtained by increasing the measured encoder value by the amount of the error term.

SYMBOL	DESCRIPTION	AVERAGE VALUE
C1	X encoder bias	+.014 ±.001
*C2	X deflection coefficient (optical to encoder axes)	-.024
*C3	X deflection offset (optical to encoder axis)	-12.265
*C4	X deflection coefficient (r-f to optical axes)	+.065 ±.005
C5	Tilt component of the north end of the X axis in an upward direction (a negative sign means tilt is down)	+.001 ±.000
C6	Tilt component of the north end of the X axis in an eastward direction (a negative sign means tilt is westward)	+.001 ±.001
*C7	X axis to Y axis lack of orthogonality (a negative sign means S6 is added to 90°)	+.007 ±.000
*C8	R-F axis to Y axis lack of orthogonality (a negative sign means S7 is added to 90°)	-.025 ±.002 (136 mc) -.037 ±.002 (400 mc) -.012 ±.002 (1700 mc)
C9	X acceleration coefficient	-.321 ±.007
C10	R-F axis to Y encoder axis bias	-.259 ±.001 (136 mc) -.301 ±.001 (400 mc) -.295 ±.001 (1700 mc)
*C11	Y deflection coefficient (optical to encoder axes)	+.222
*C12	Y deflection offset (optical to encoder axes)	-2.579
C13	Y acceleration coefficient	-.135 ±.017
*C14	Y deflection coefficient (r-f to optical axes)	+.046 ±.005
*C15	Y hysteresis	-.001 ±.000
X(C)rms	X rms of the fit to the measured minus predicted values	+.032 (136 mc) +.027 (400 mc) +.003 (1700 mc)
Y(C)rms	Y rms of the fit to the measured minus predicted values	+.014 (136 mc) +.021 (400 mc) +.007 (1700 mc)

TABLE 2-3. TEST ANALYSIS

*The deflection terms, hysteresis, and orthogonality require additional explanation. The r-f to encoder deflection is just the sum of the Star Shot and Aircraft track deflection, as shown in the error equations. Y hysteresis and axis orthogonality sign conventions are described in the Star Shot table.

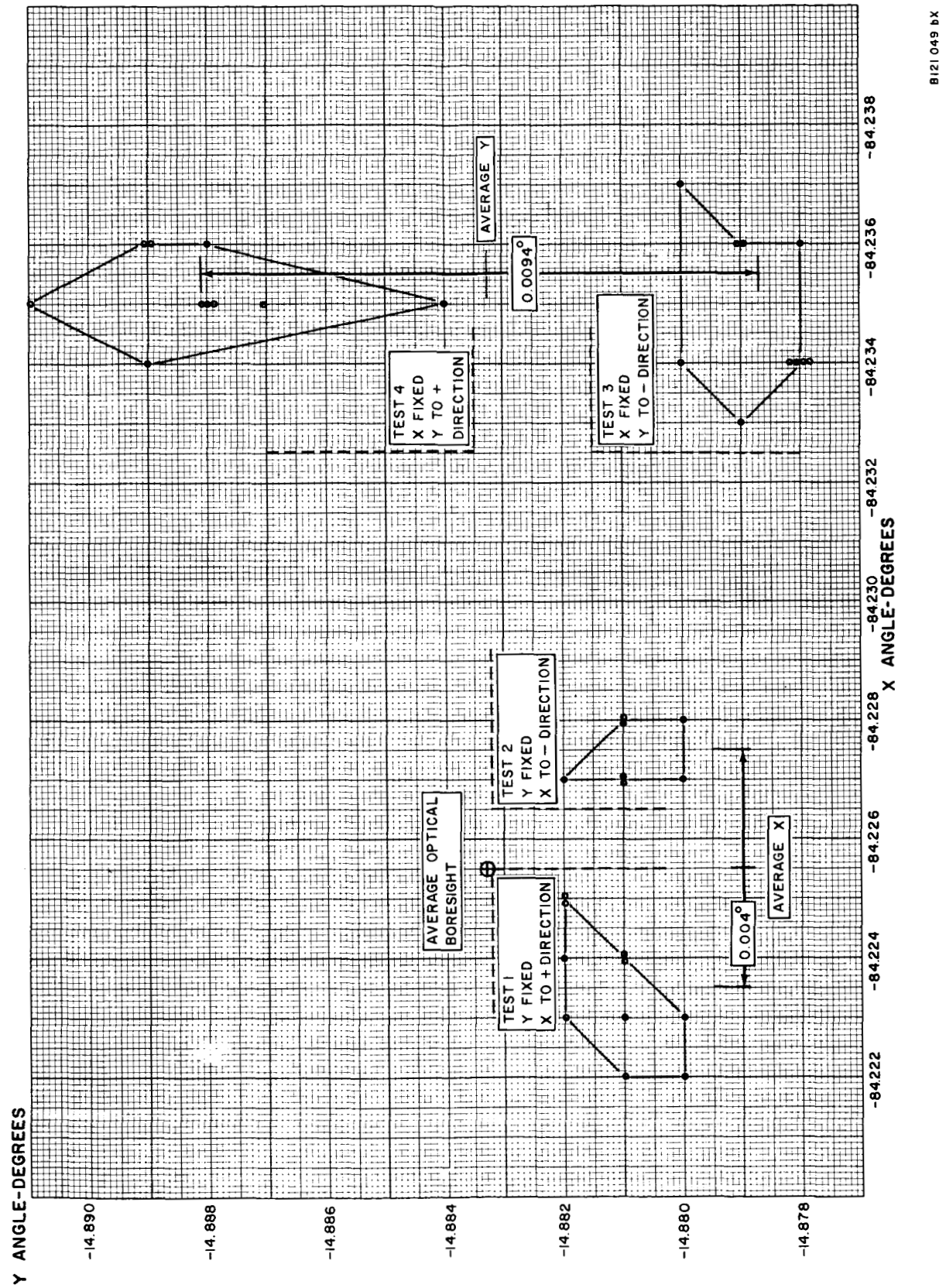

Figure 2-1. Optical Boresight Test

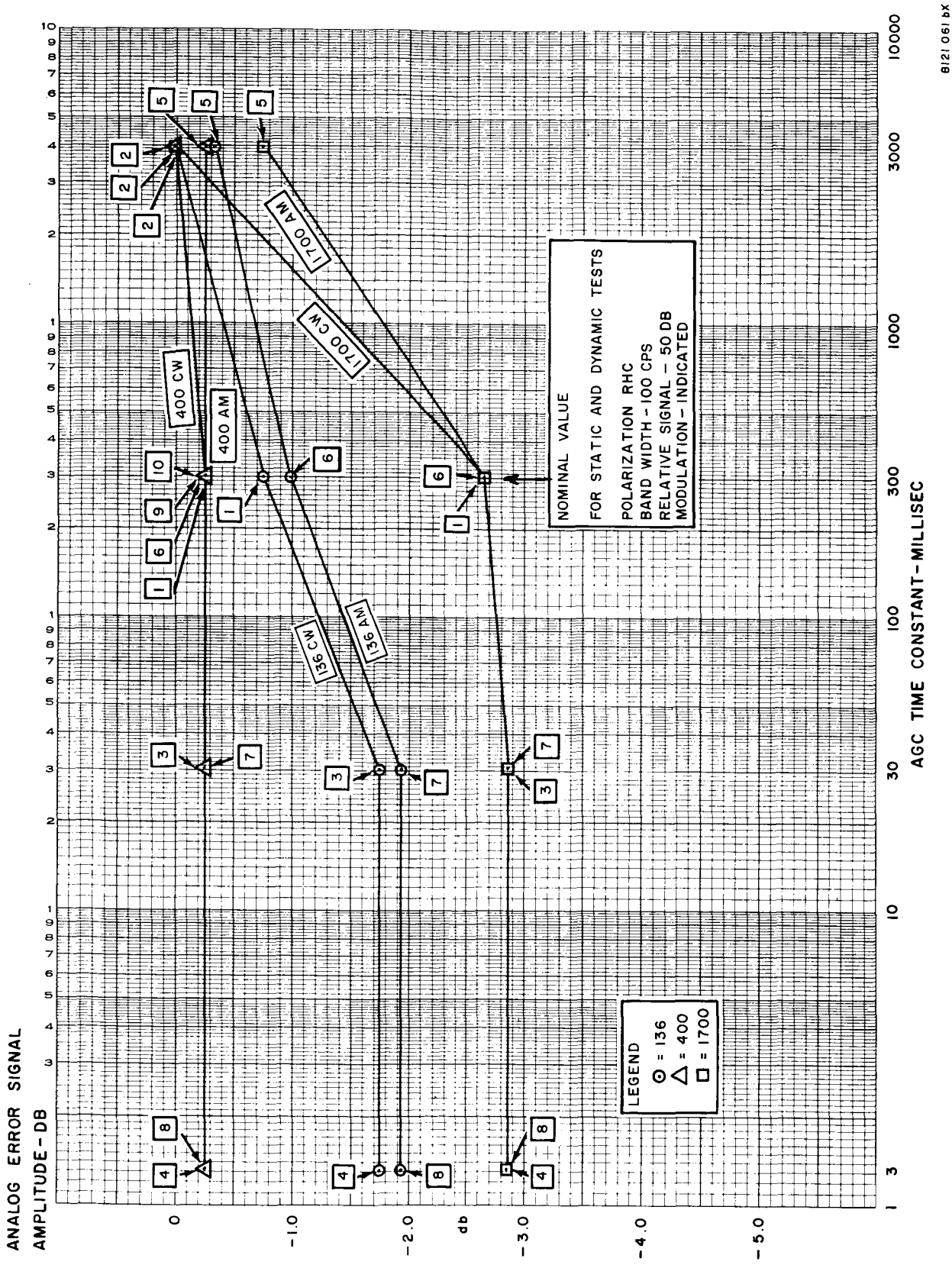

Figure 2-2. Receiver Analog Error Signal Versus AGC Time

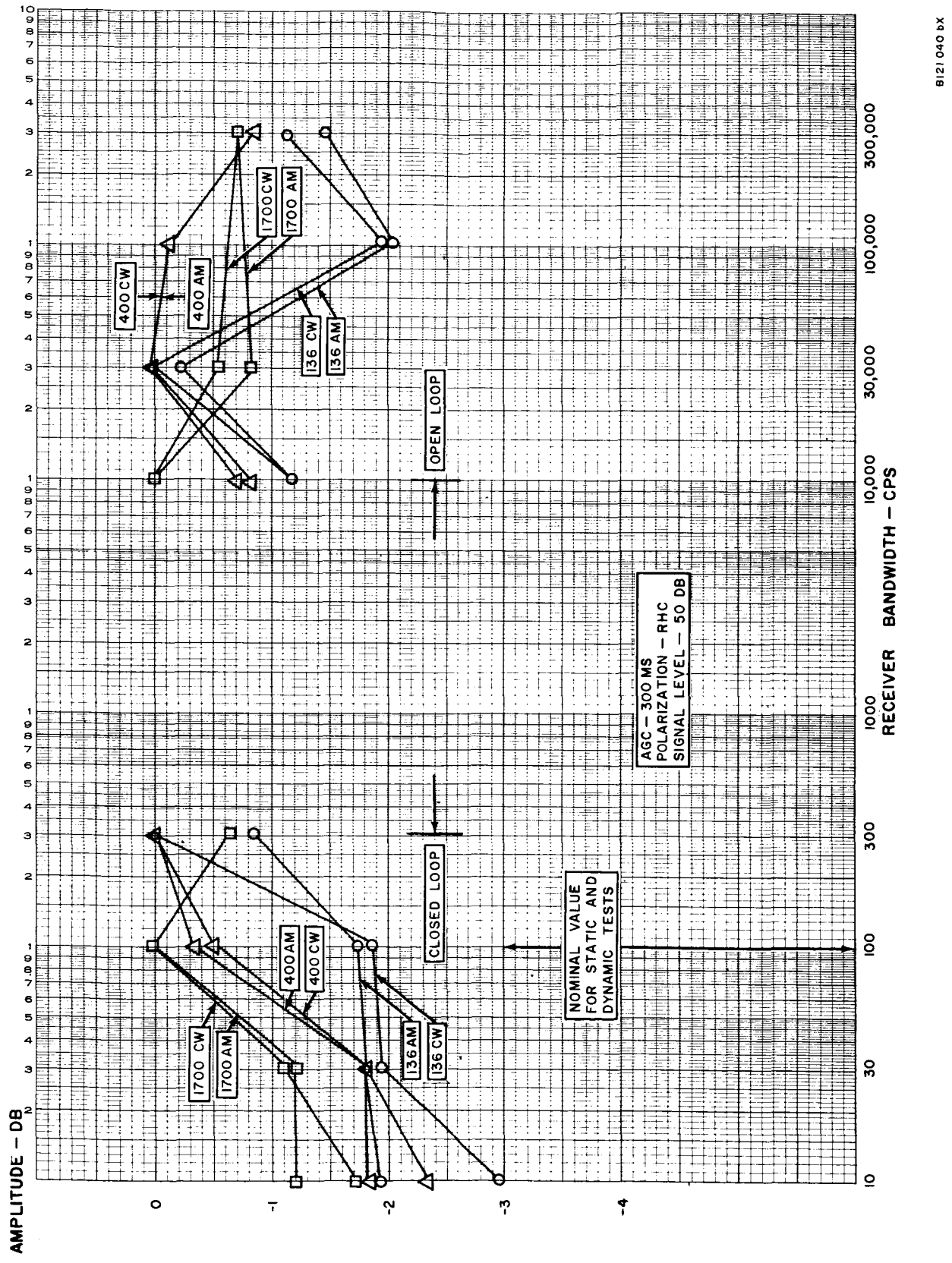

Figure 2-3. Receiver Analog Error Signal Versus Receiver Bandwidth

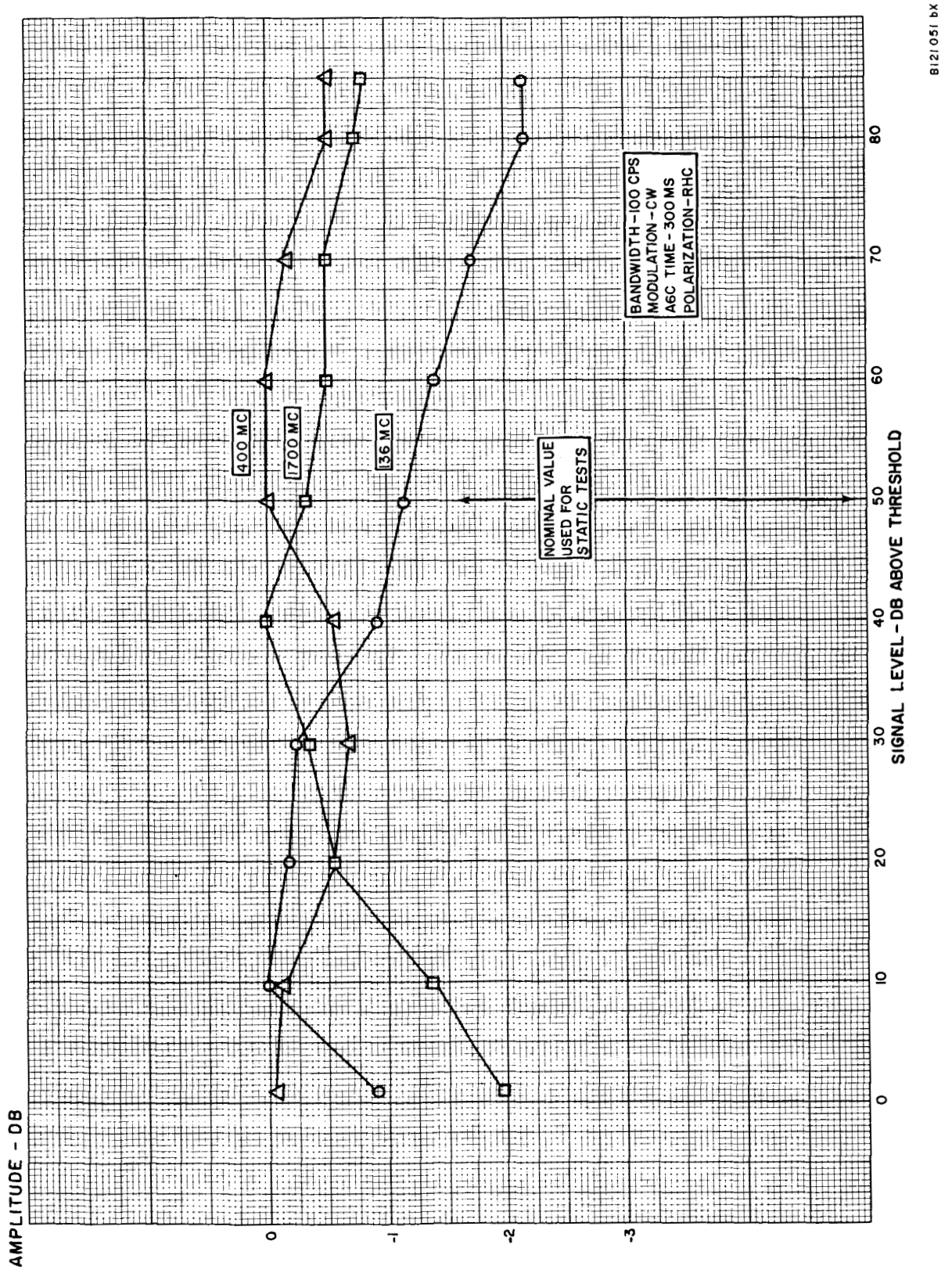

Figure 2-4. Receiver Analog Error Signals Versus Signal Level

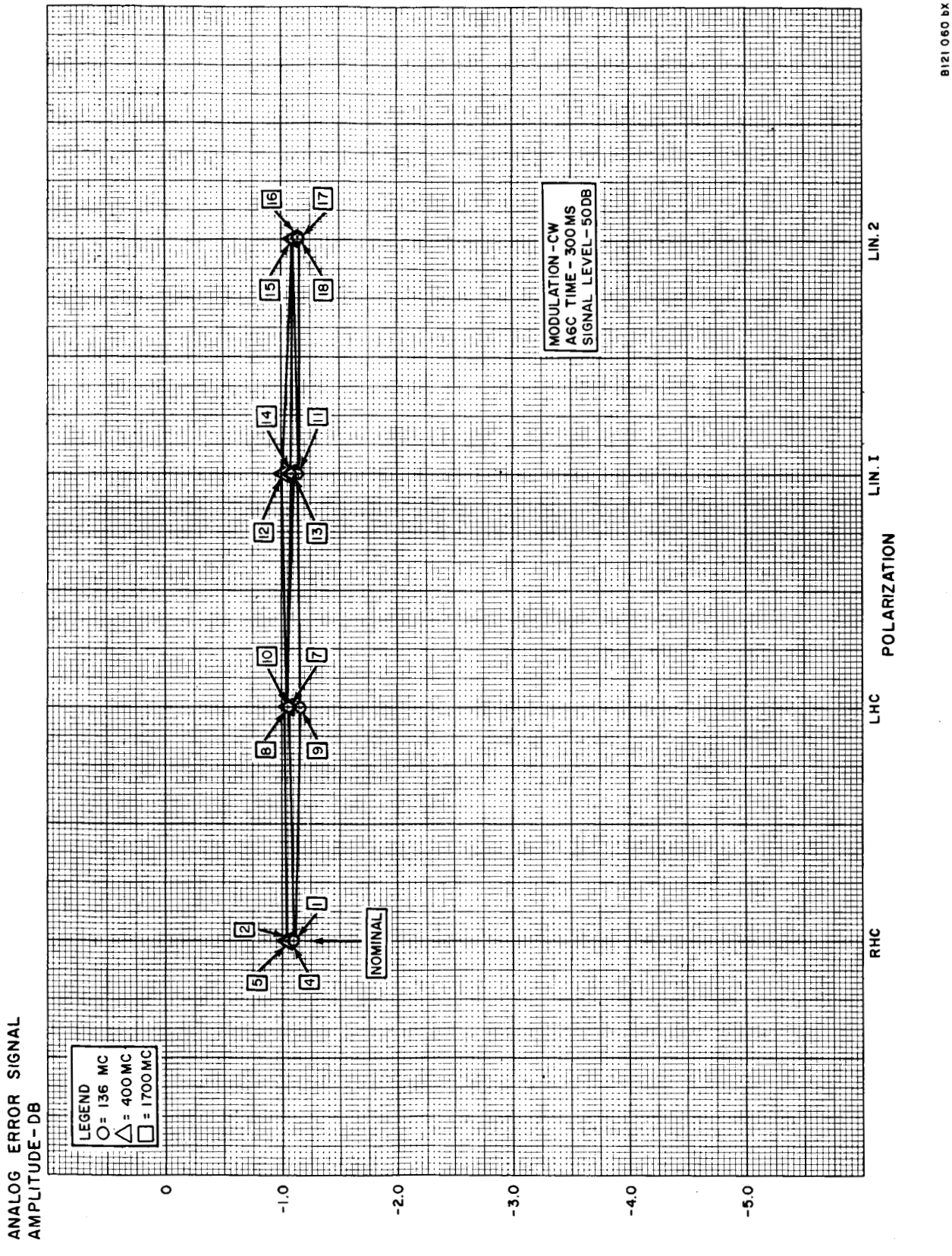

Figure 2-5. Receiver Analog Error Signal Versus Polarization

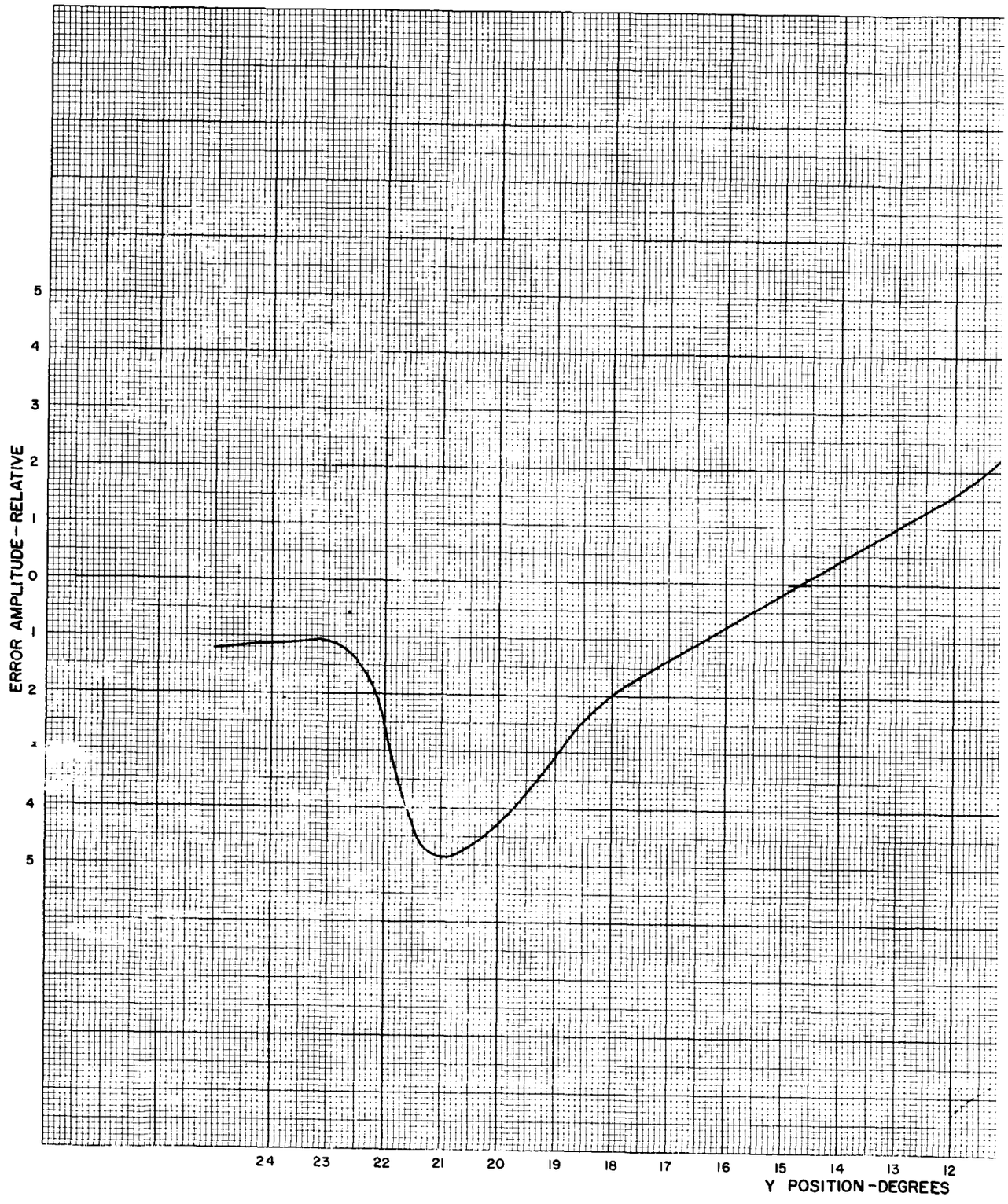
ERROR AMPLITUDE - RELATIVE
5
4
3
2
1
0
1
2
4
5
24
23
22
21
20
19
18
17
16
15
14
13
12
Y POSITION - DEGREES

2-25-1

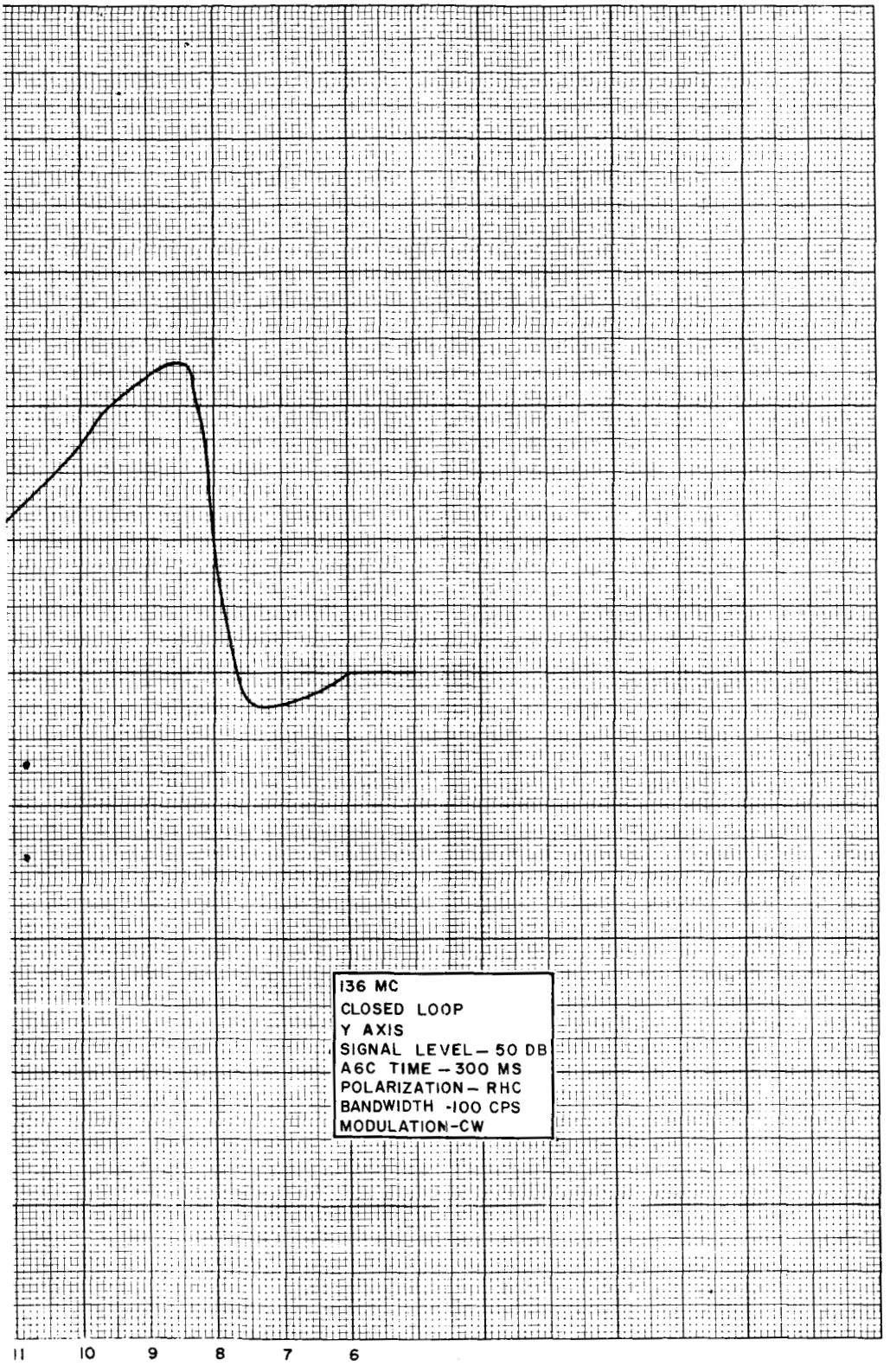

Figure 2-6. Receiver Analog Error Signal, Typical Analog Curve

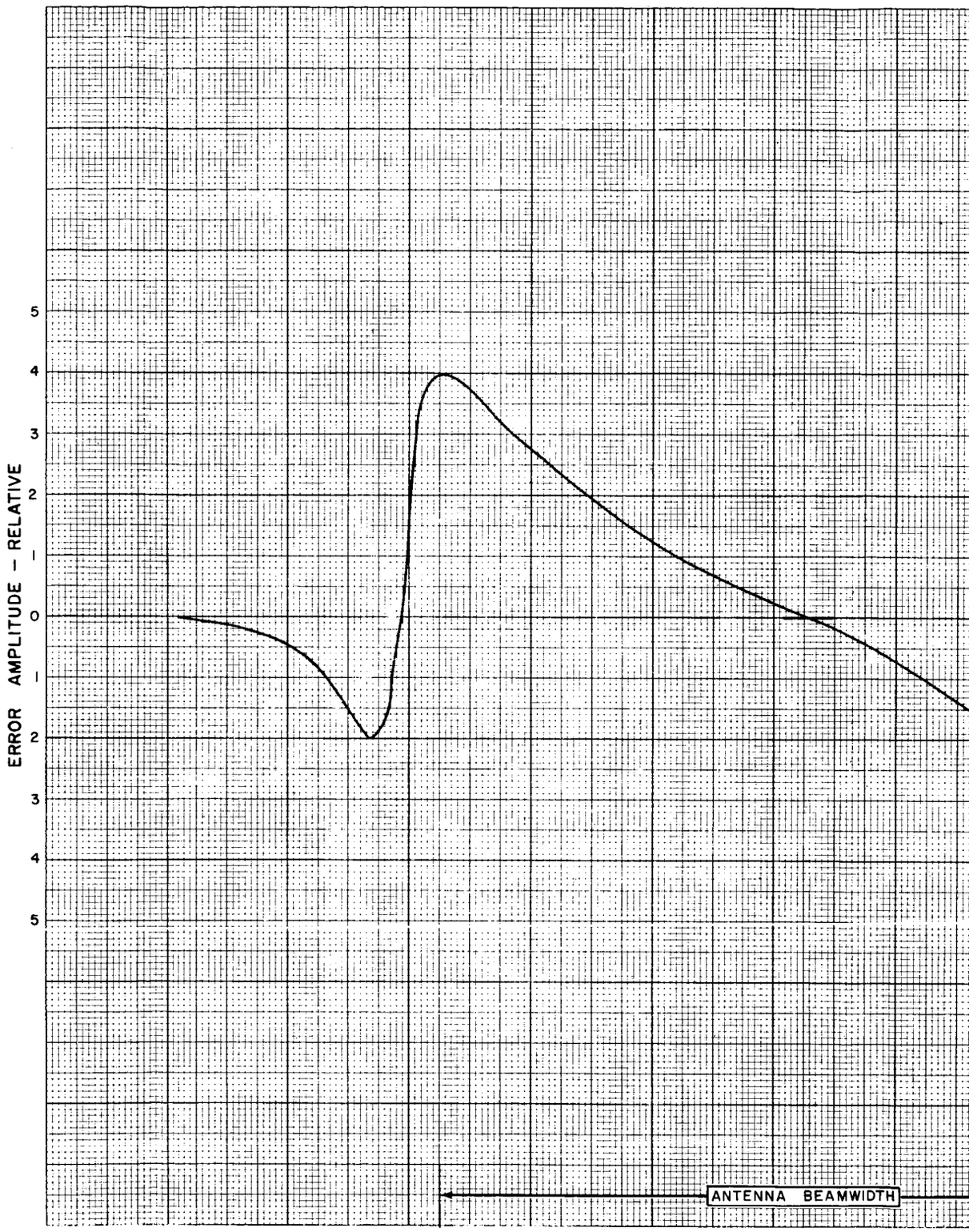
ERROR AMPLITUDE – RELATIVE
5
4
3
2
1
0
1
2
3
4
5
ANTENNA BEAMWIDTH
6
7
8
9
10
11
12
13
14
15
16
17
Y POSITION –

2-26-1

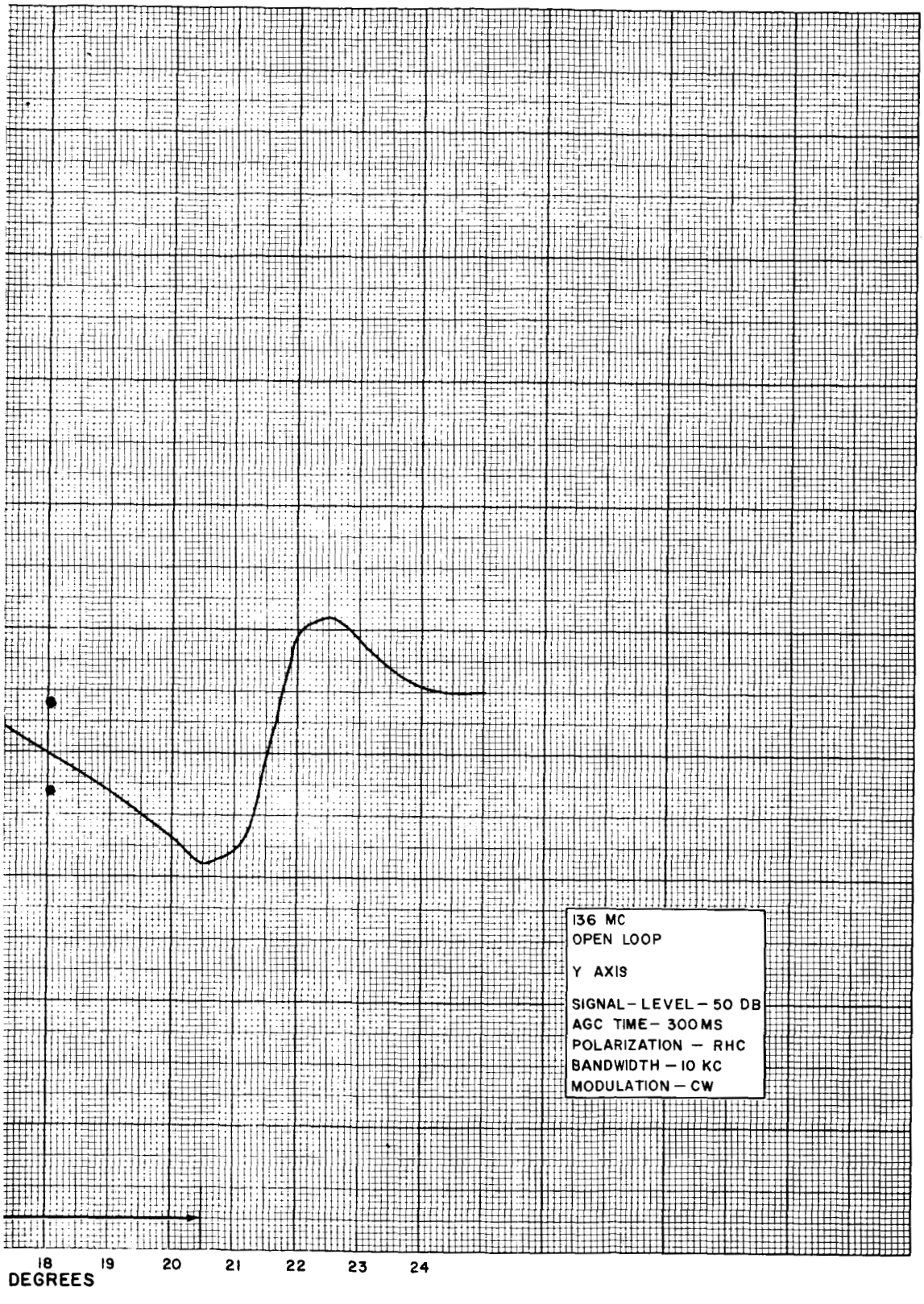

8121 034 cX

Figure 2-7. Receiver Analog Error Signals, Typical Analog Curve 136-Mc Open Loop, Y-Axis

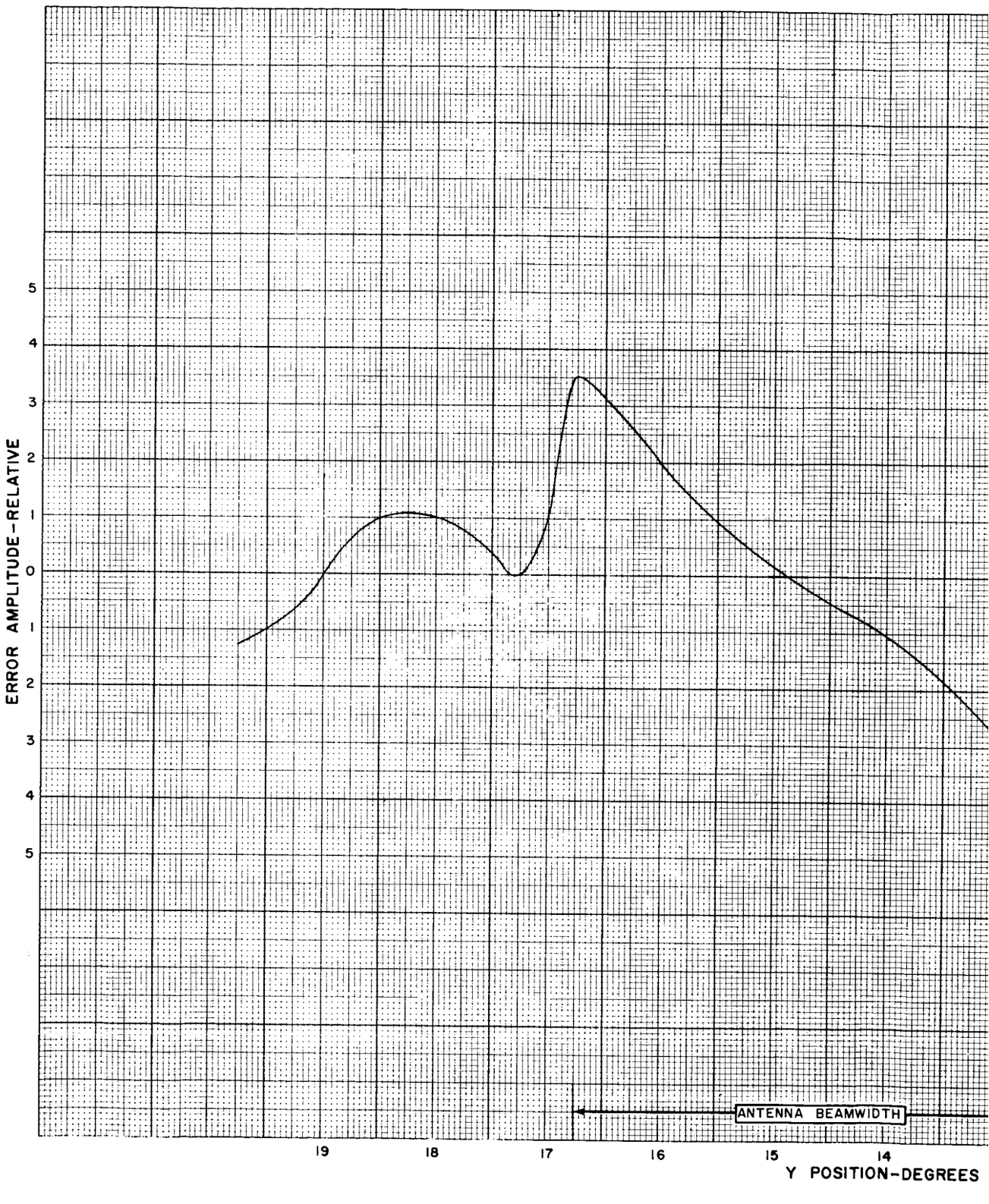
ERROR AMPLITUDE-RELATIVE
5
4
3
2
1
0
1
2
3
4
5
ANTENNA BEAMWIDTH
19
18
17
16
15
14
Y POSITION-DEGREES

2-27-1

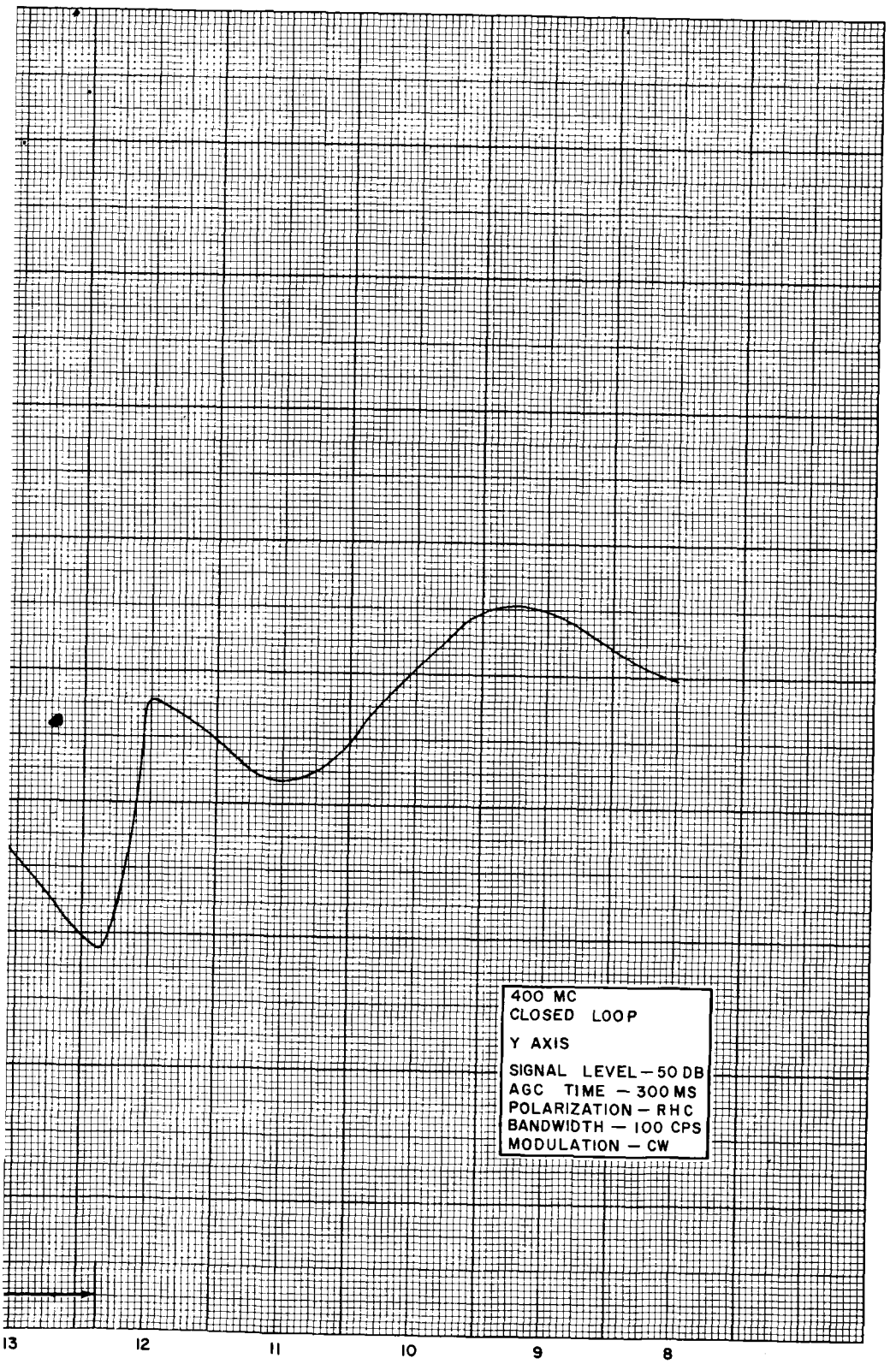

B121 035 cX

Figure 2-8. Receiver Analog Error Signals, Typical Analog Curves 400-Mc Closed Loop, Y-Axis

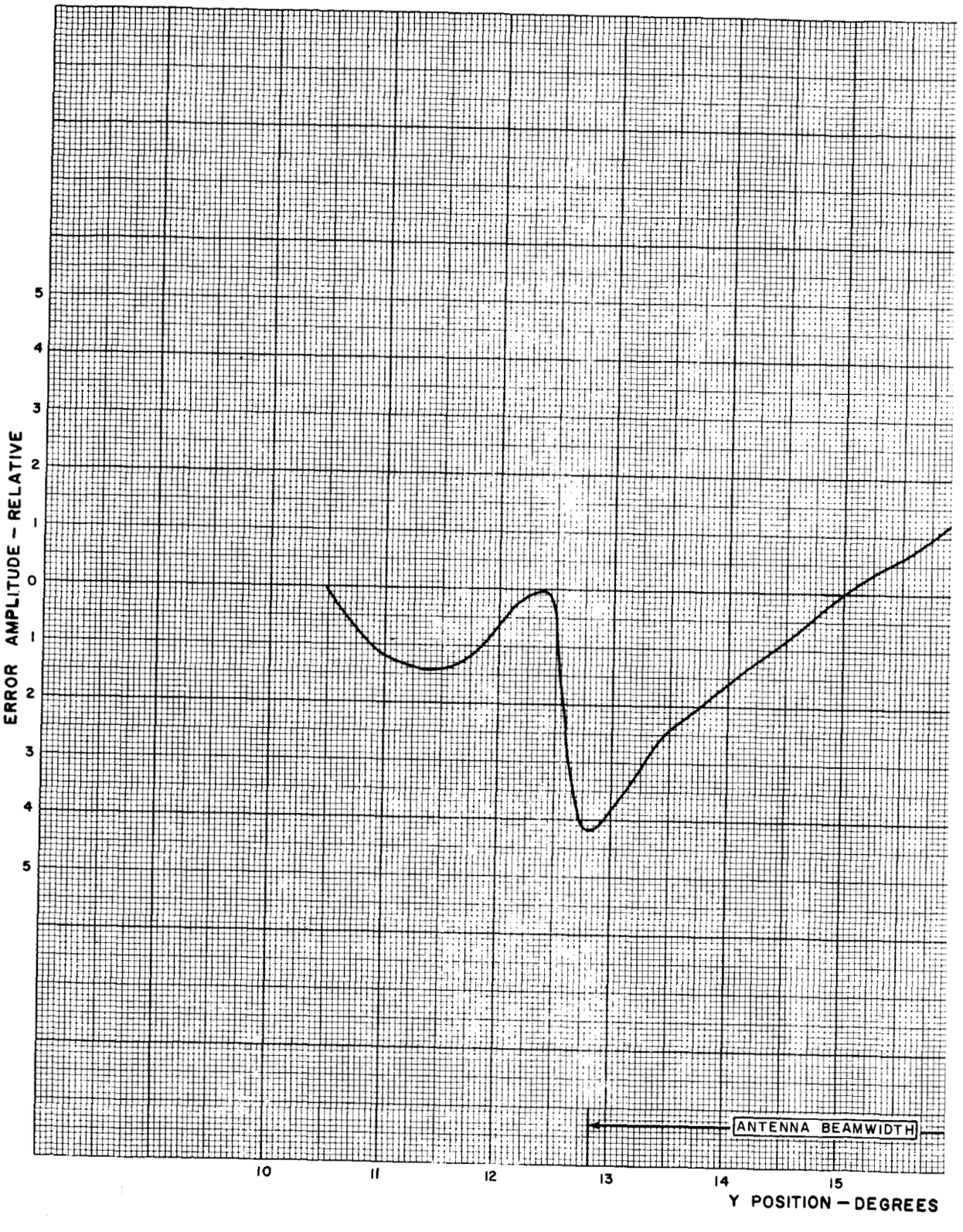
ERROR AMPLITUDE – RELATIVE
5
4
3
2
1
0
1
2
3
4
5
ANTENNA BEAMWIDTH
10
11
12
13
14
15
Y POSITION – DEGREES

2-28-1

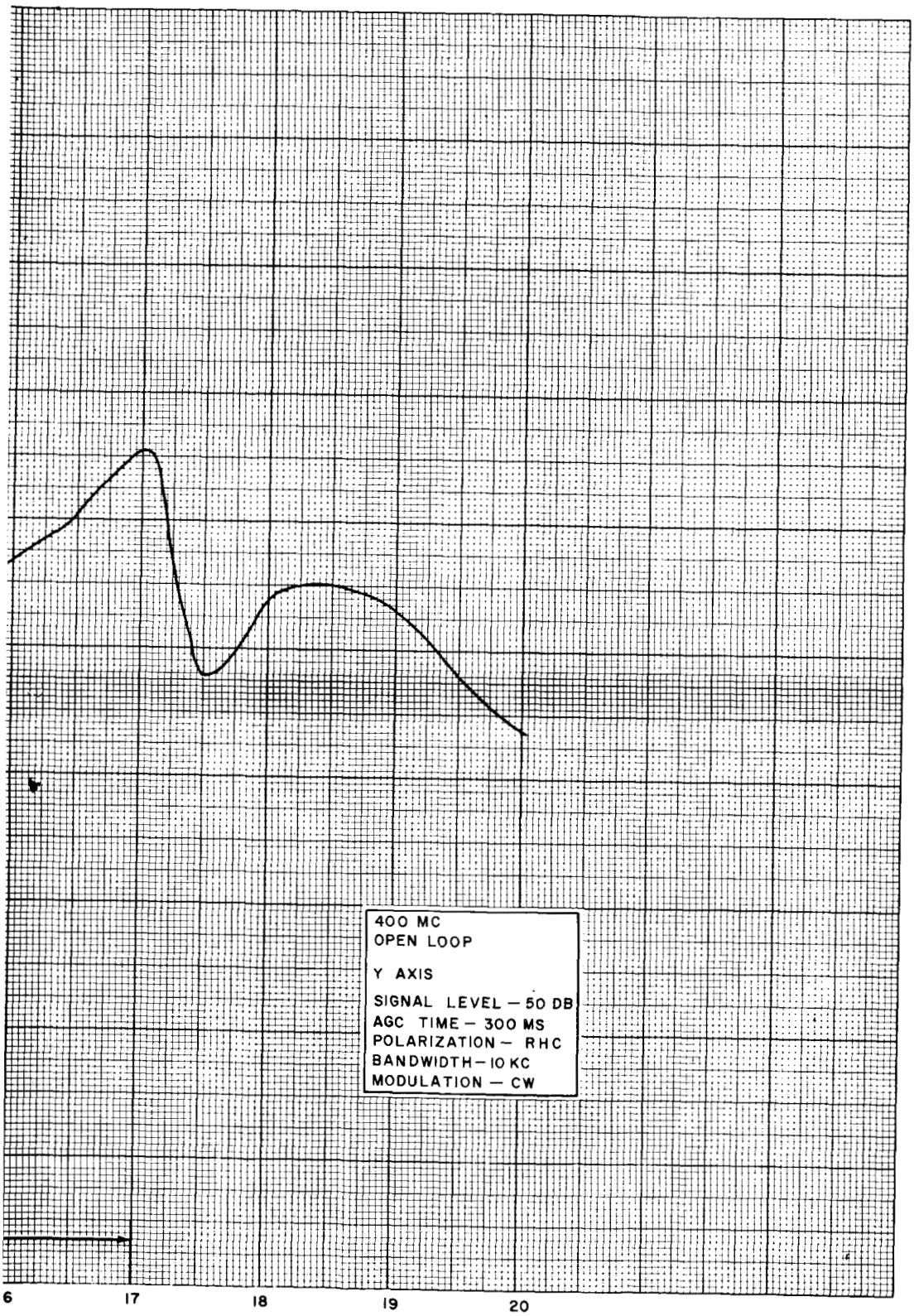

B121 036 cX

Figure 2-9. Receiver Analog Error Signal, Typical Analog Curve 400-Mc Open Loop, Y-Axis

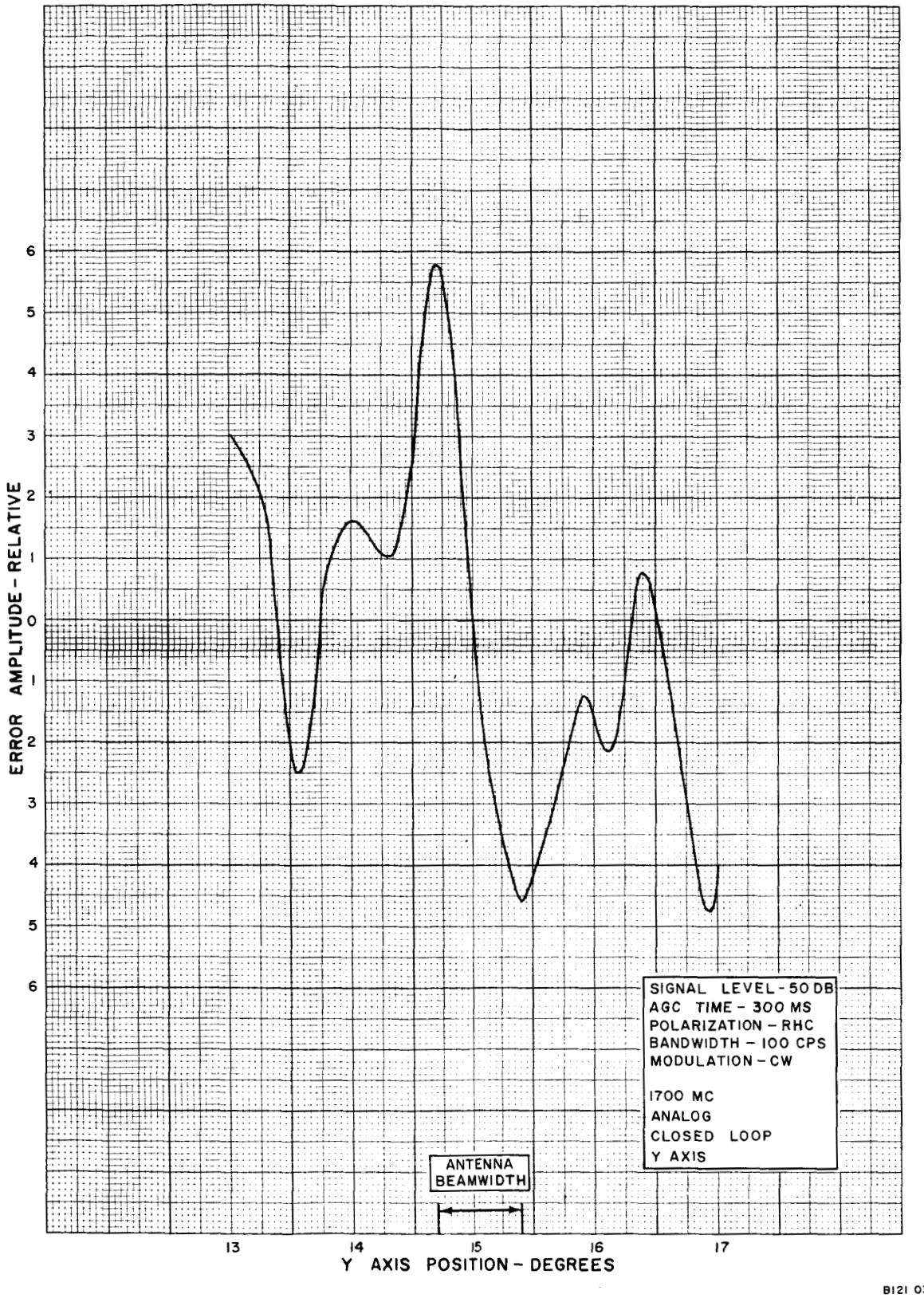

Figure 2-10. Receiver Analog Error Signal, Typical Analog Curve 1700-Mc Closed Loop, Y Axis

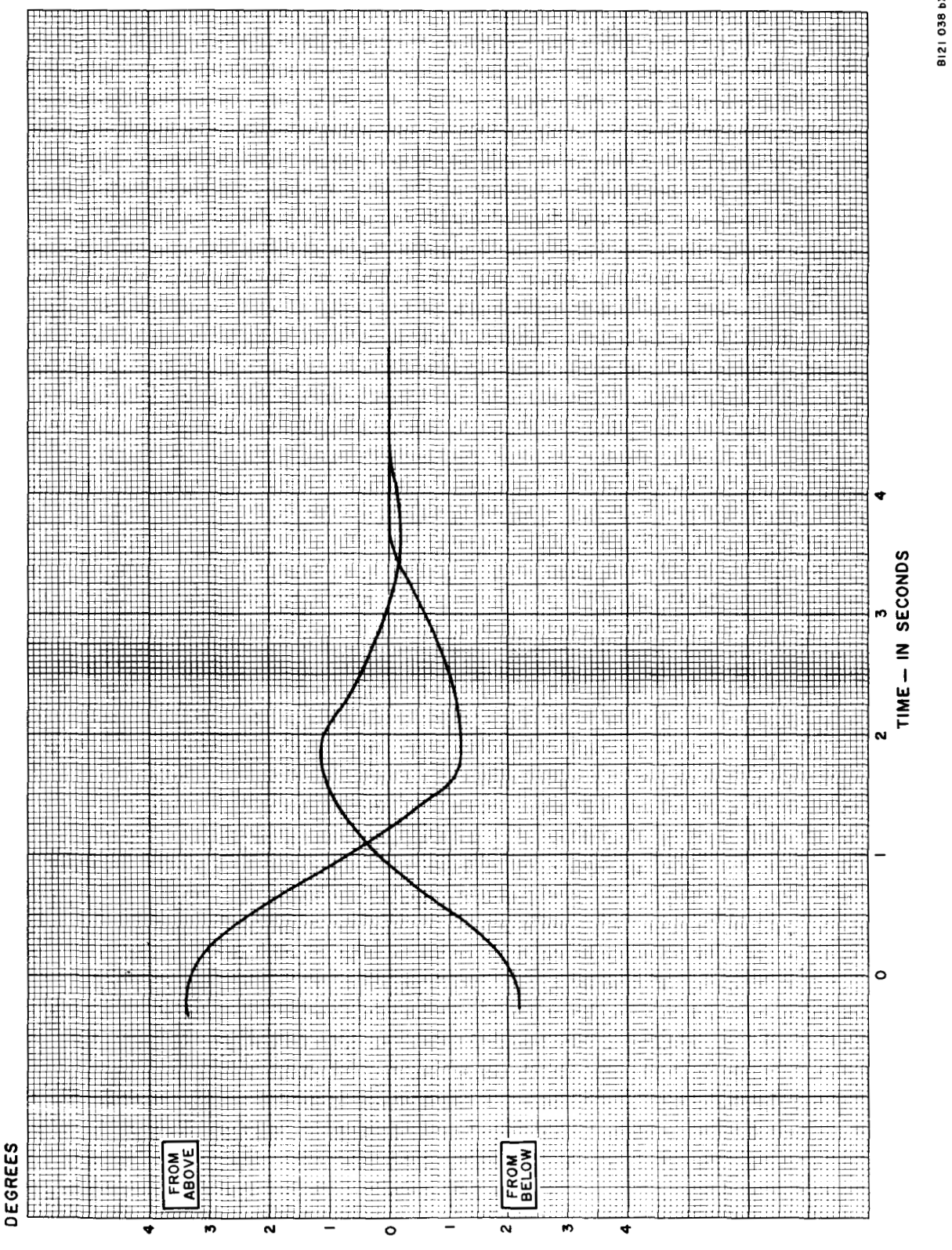

Figure 2-11. Static Acquisition, 136-Mc Snap-On, X-Axis

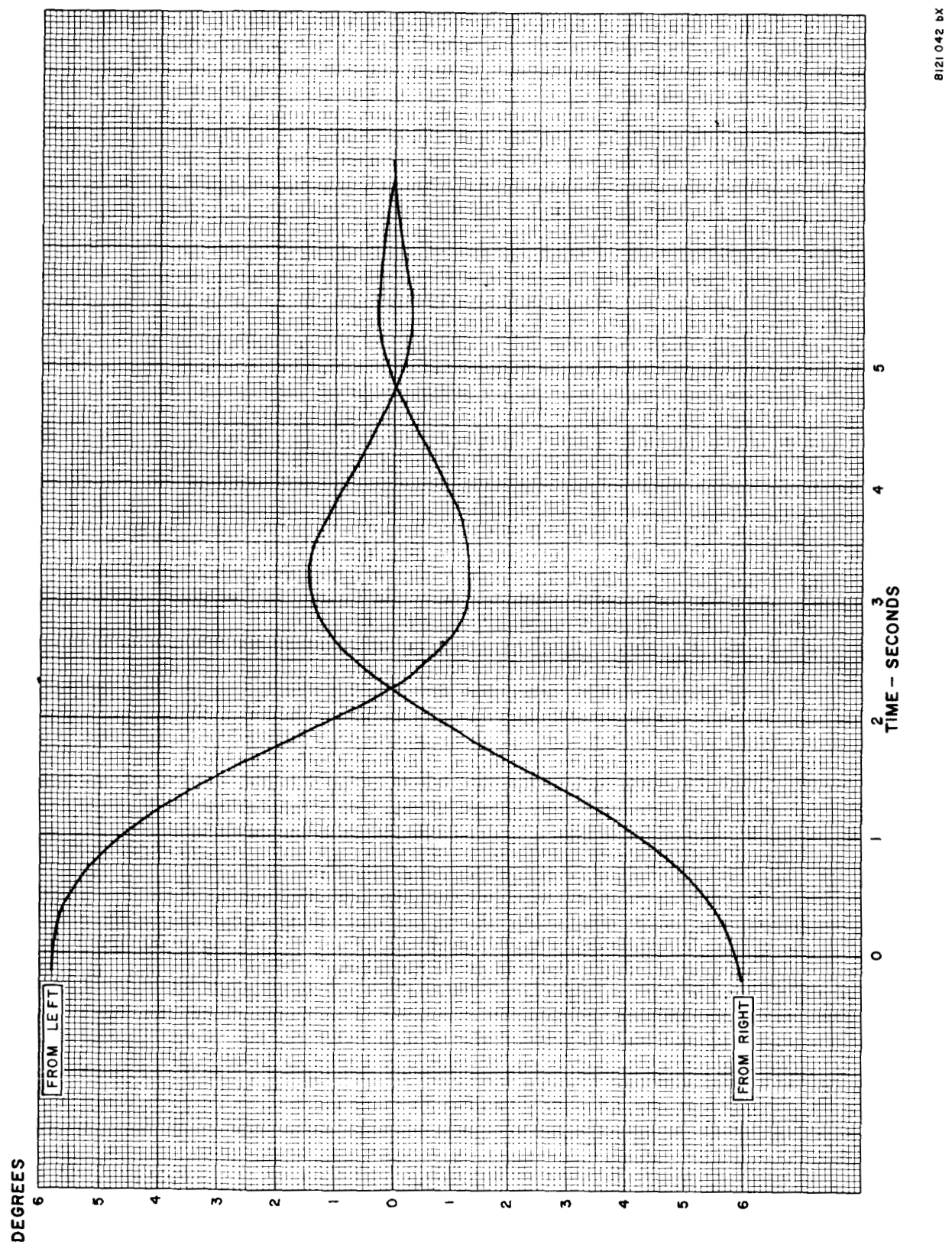

Figure 2-12. Static Acquisition, 136-Mc Snap-On, Y-Axis

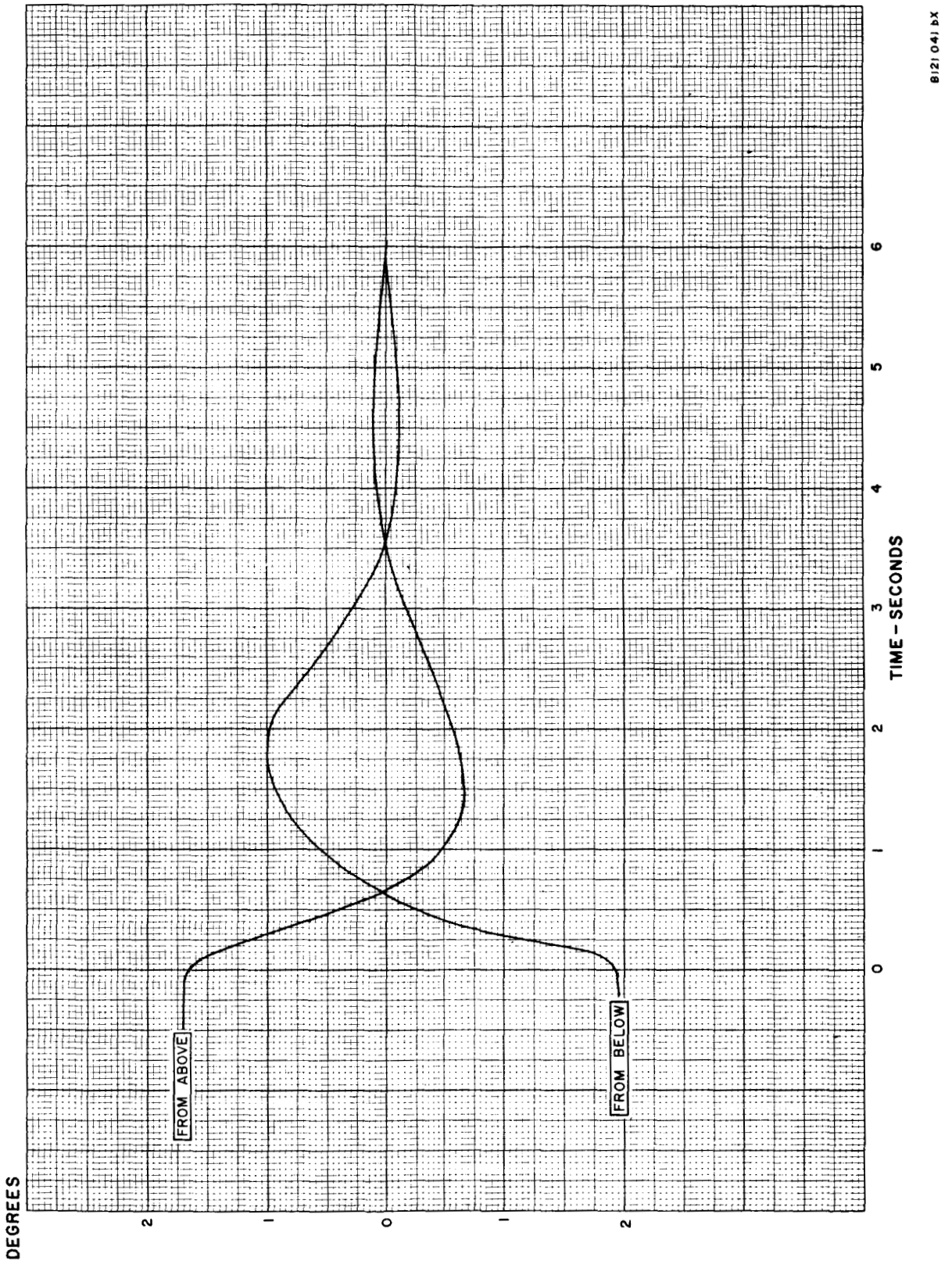

Figure 2-13. Static Acquisition, 400-Mc Snap-On, X-Axis

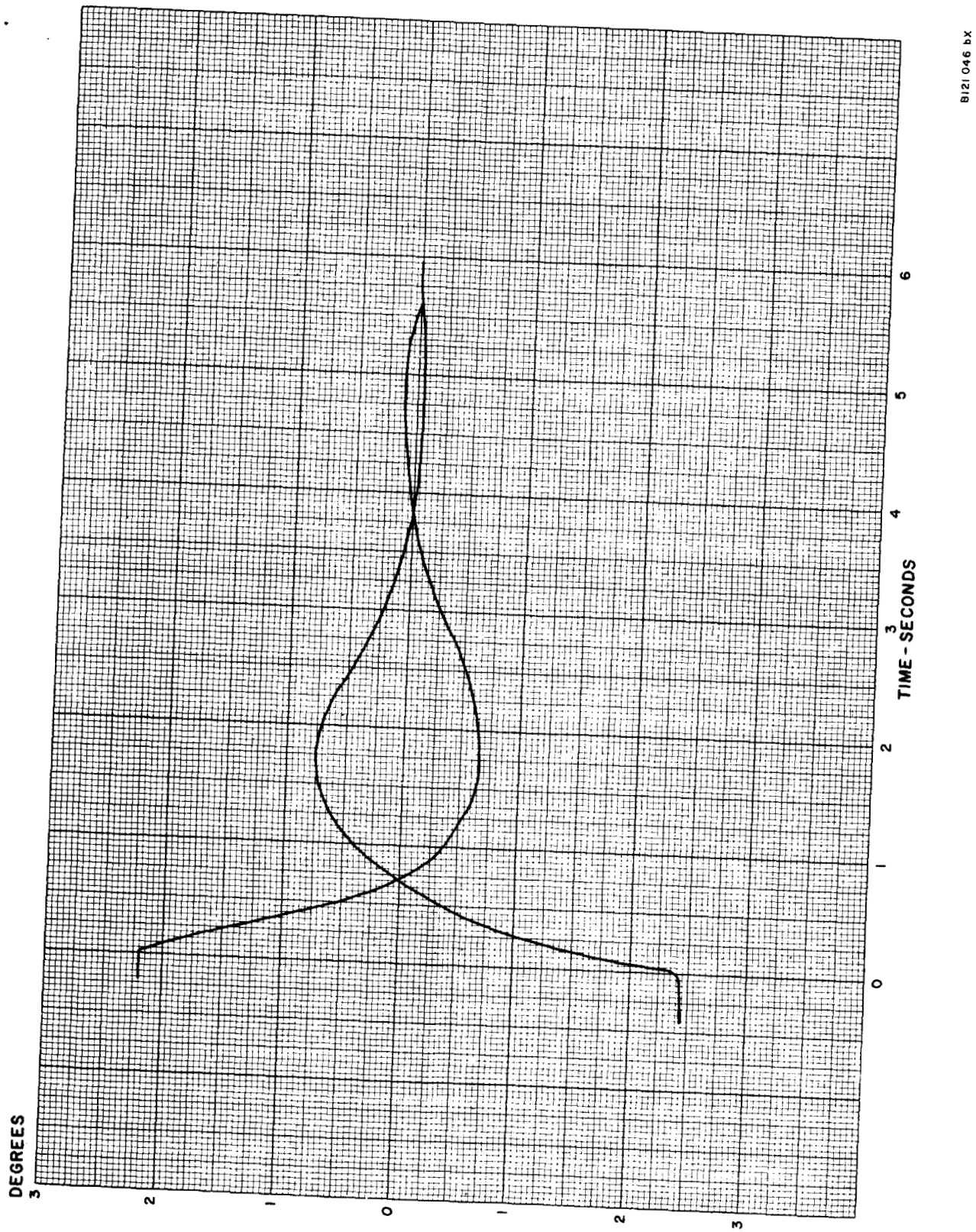

Figure 2-14. Static Acquisition, 400-Mc Snap-On, Y-Axis

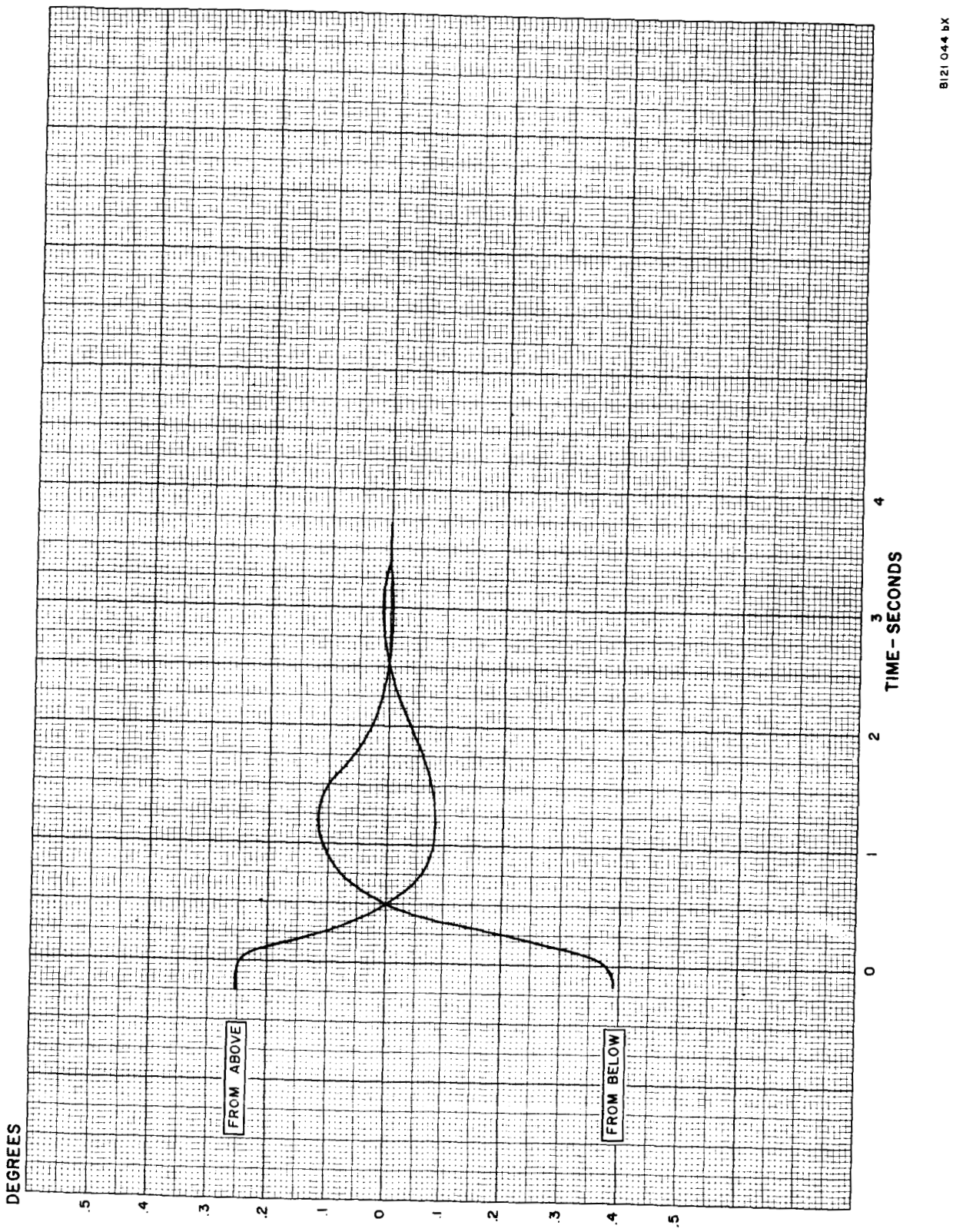

Figure 2-15. Static Acquisition, 1700-Mc Snap-On, X-Axis

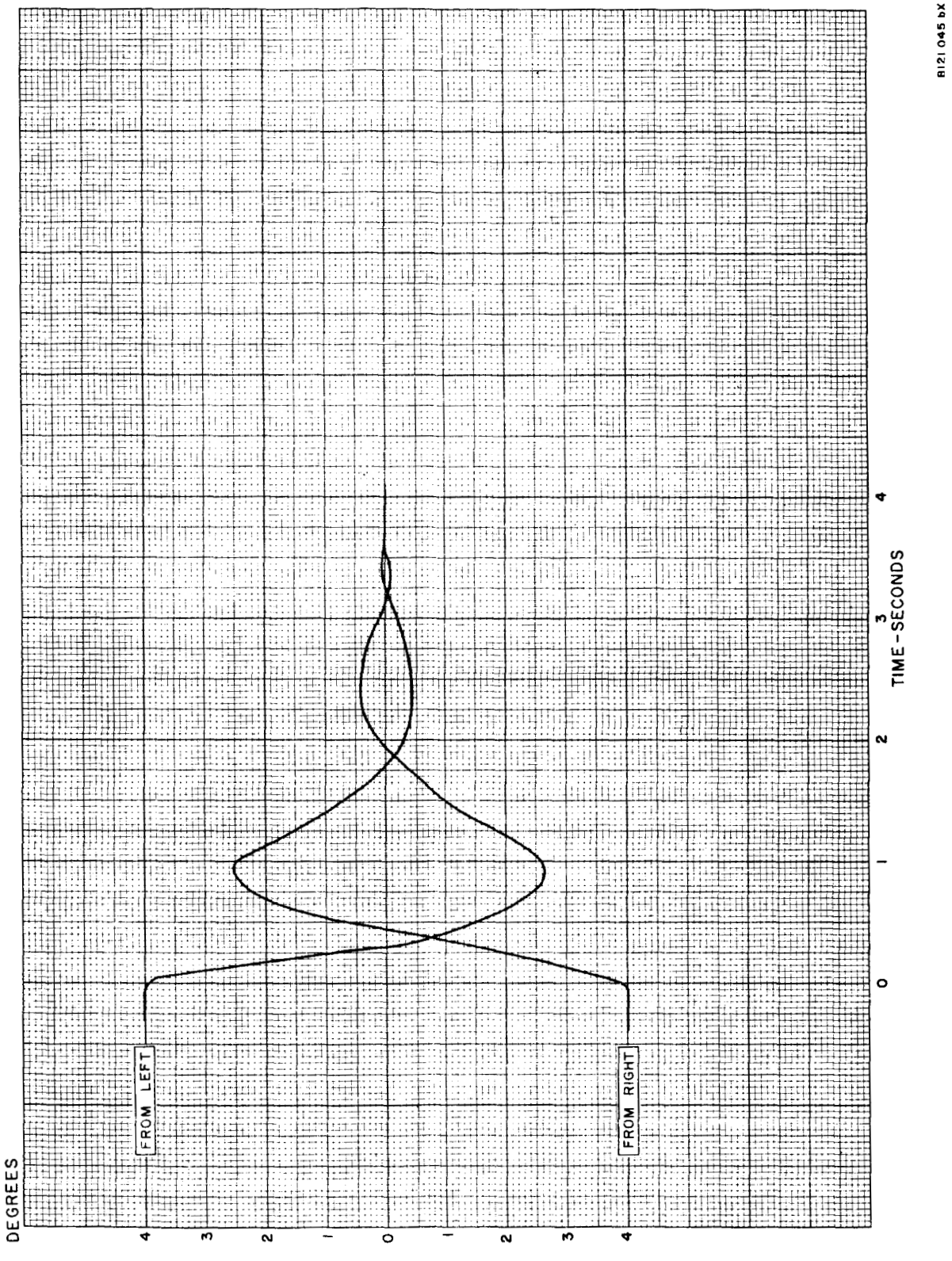

Figure 2-16. Static Acquisition, 1700-Mc Snap-On, Y-Axis

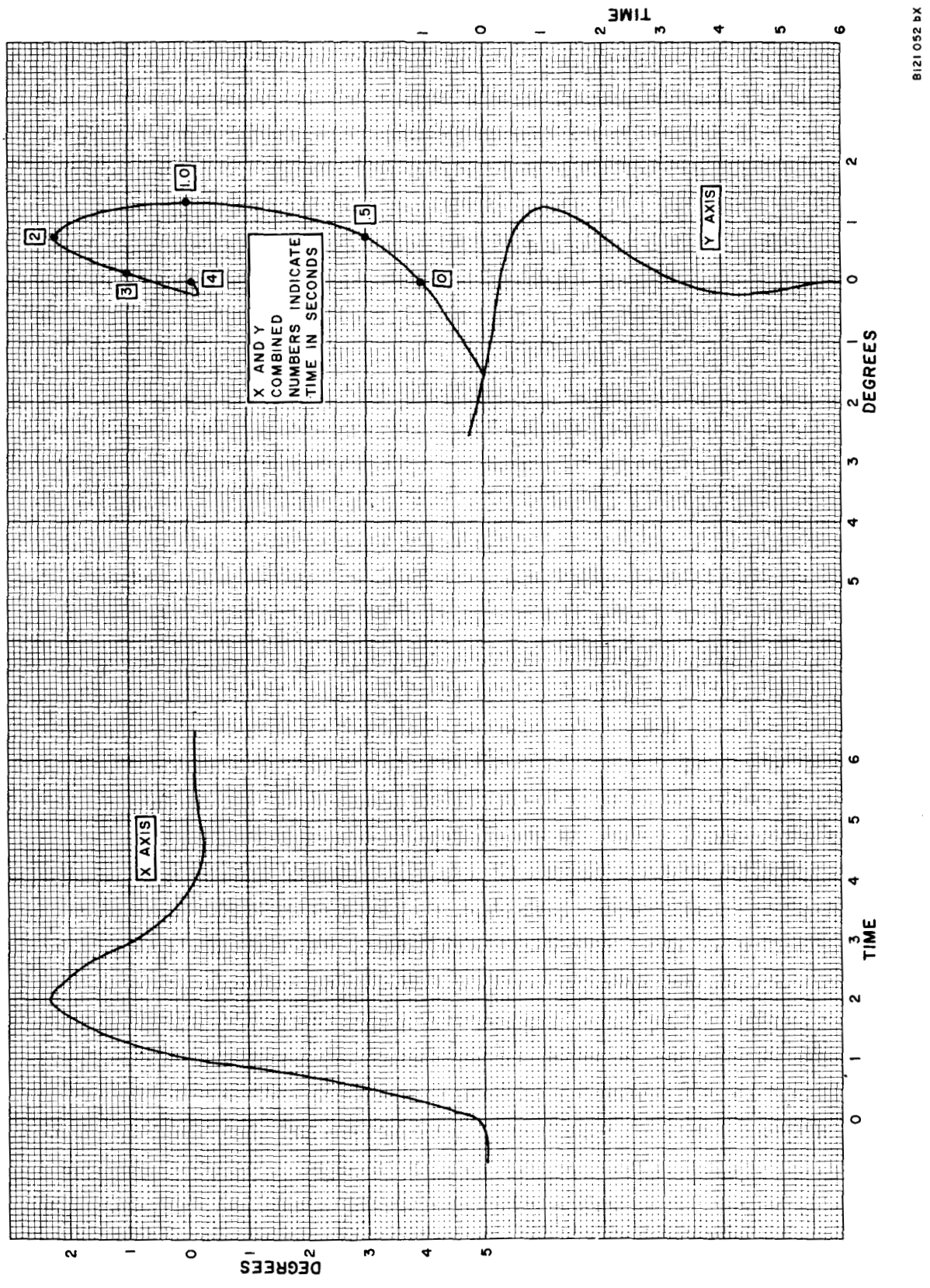

Figure 2-17. Static Acquisition, 400-Mc Snap-On, Both Axes

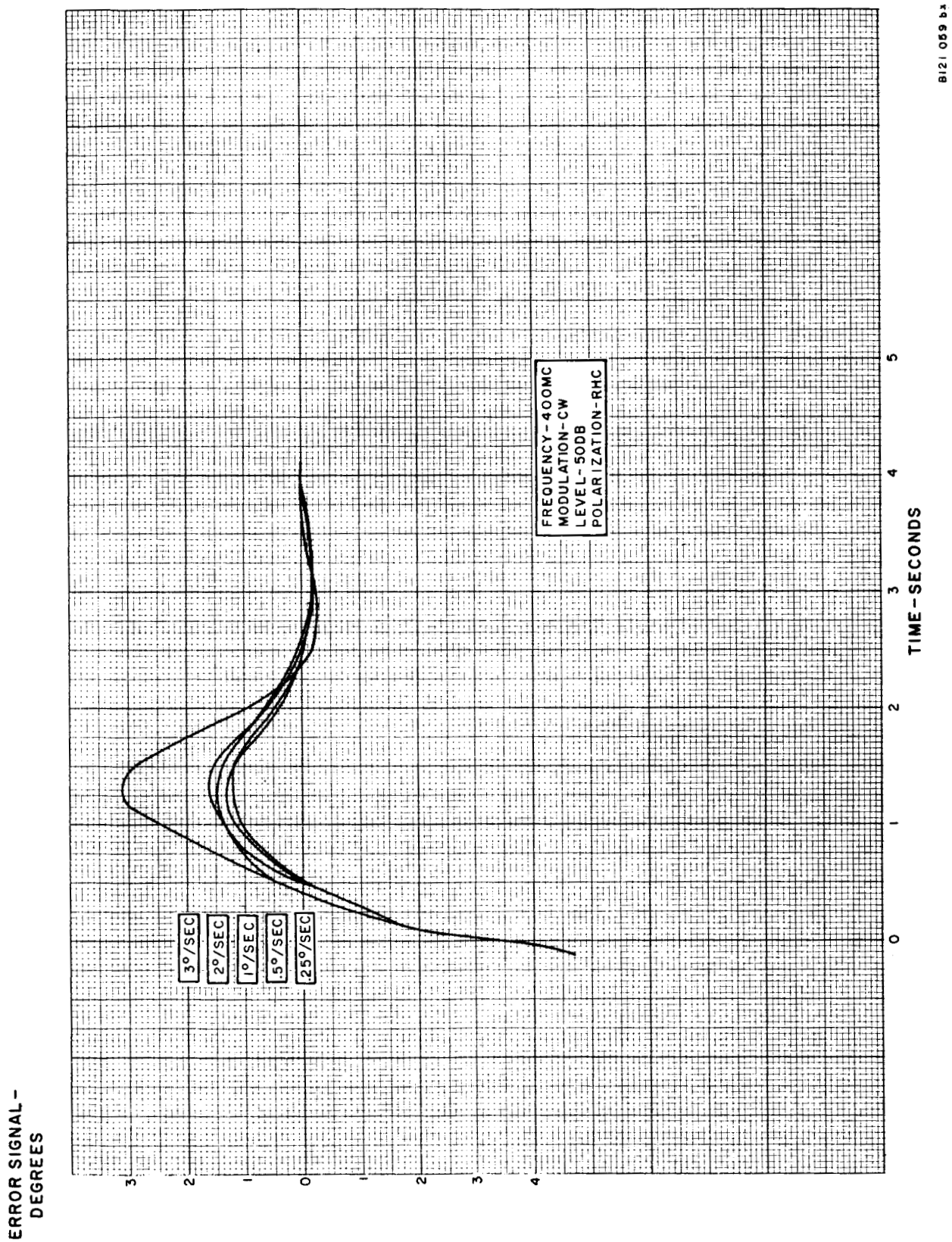

Figure 2-18. Acquisition From Initial Velocity

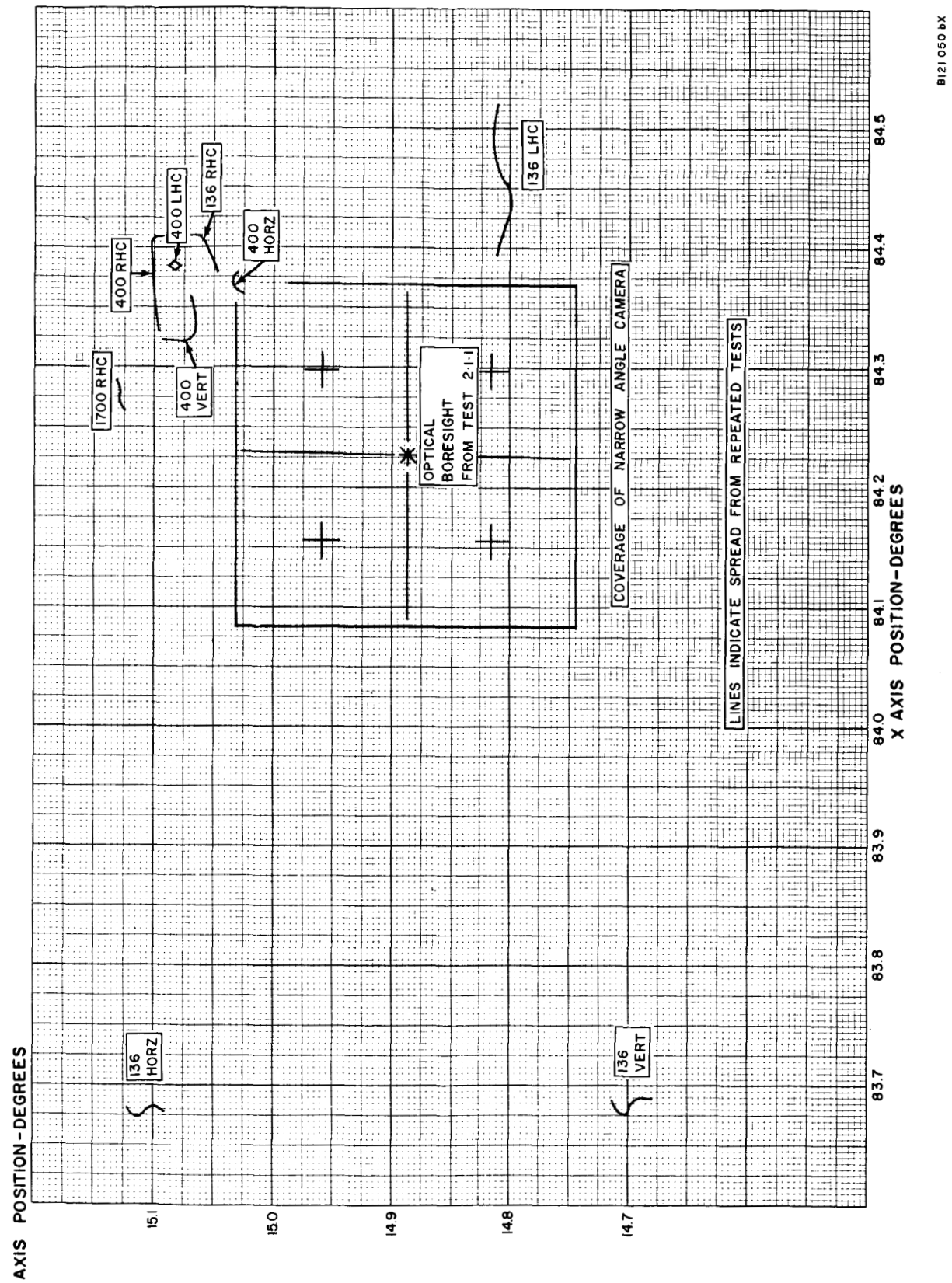

Figure 2-19. R-F Boresight

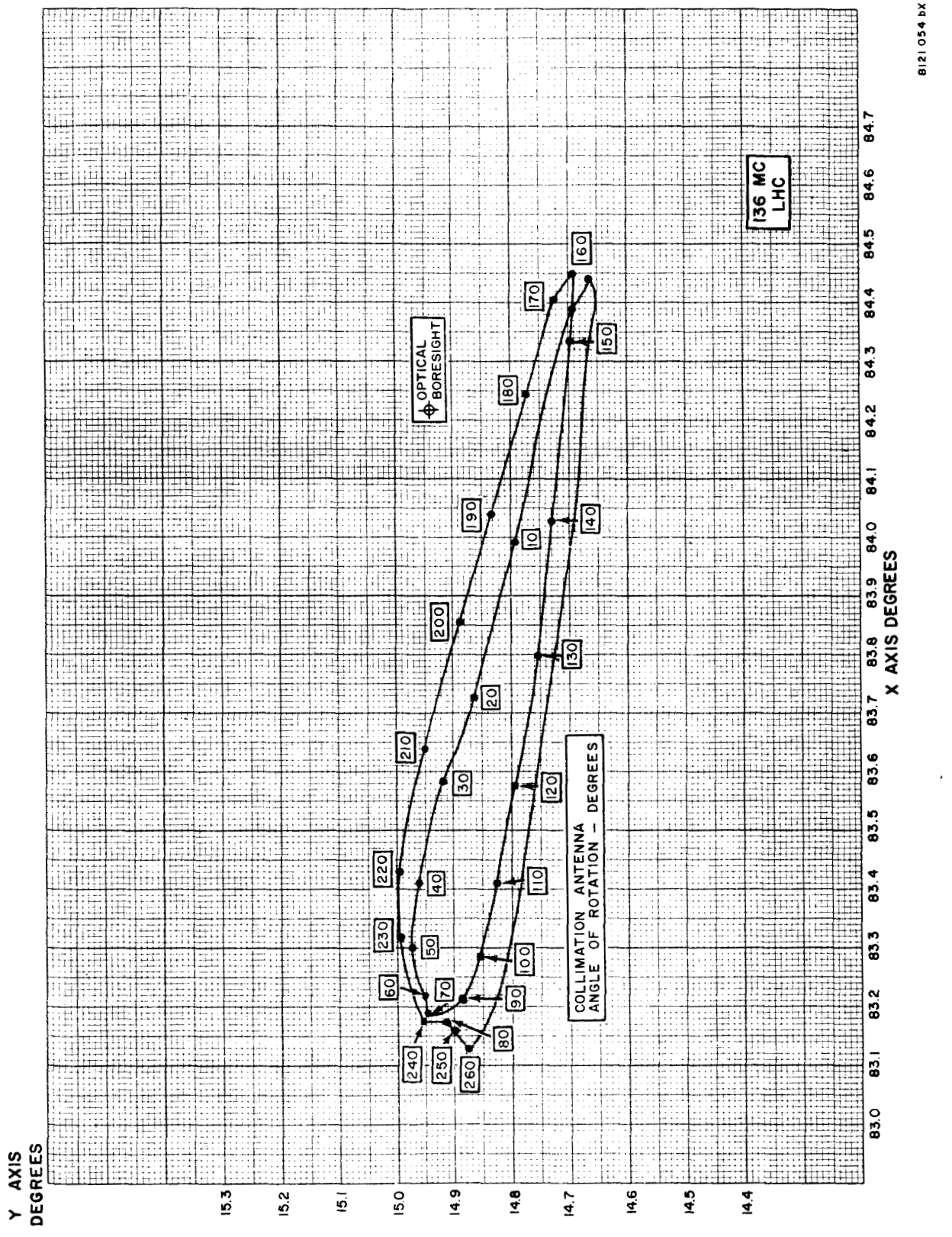

Figure 2-20. R-F Boresight Shift With Polarization (136-Mc LHC)

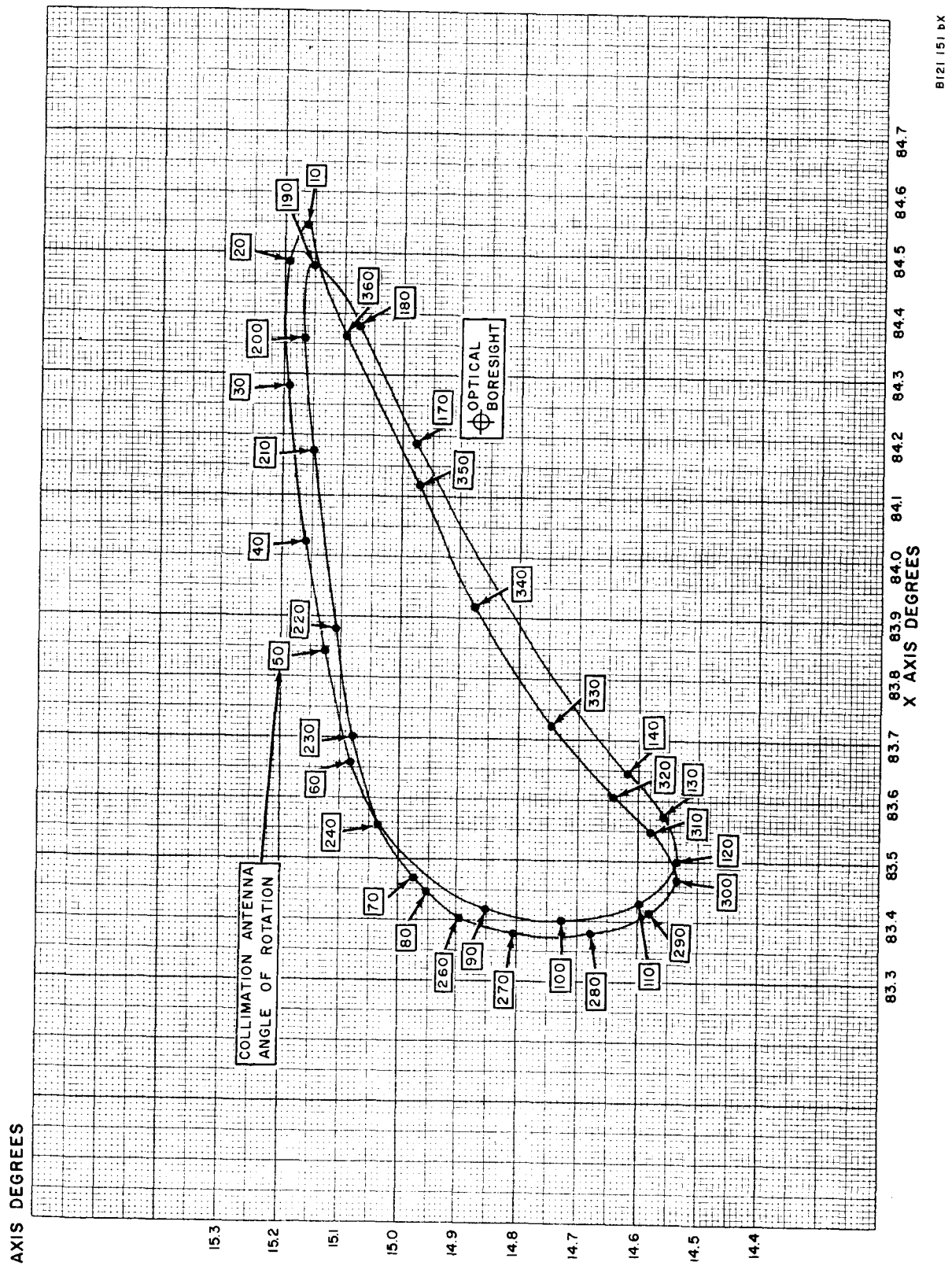

Figure 2-21. R-F Boresight with Polarization, 136 Mc

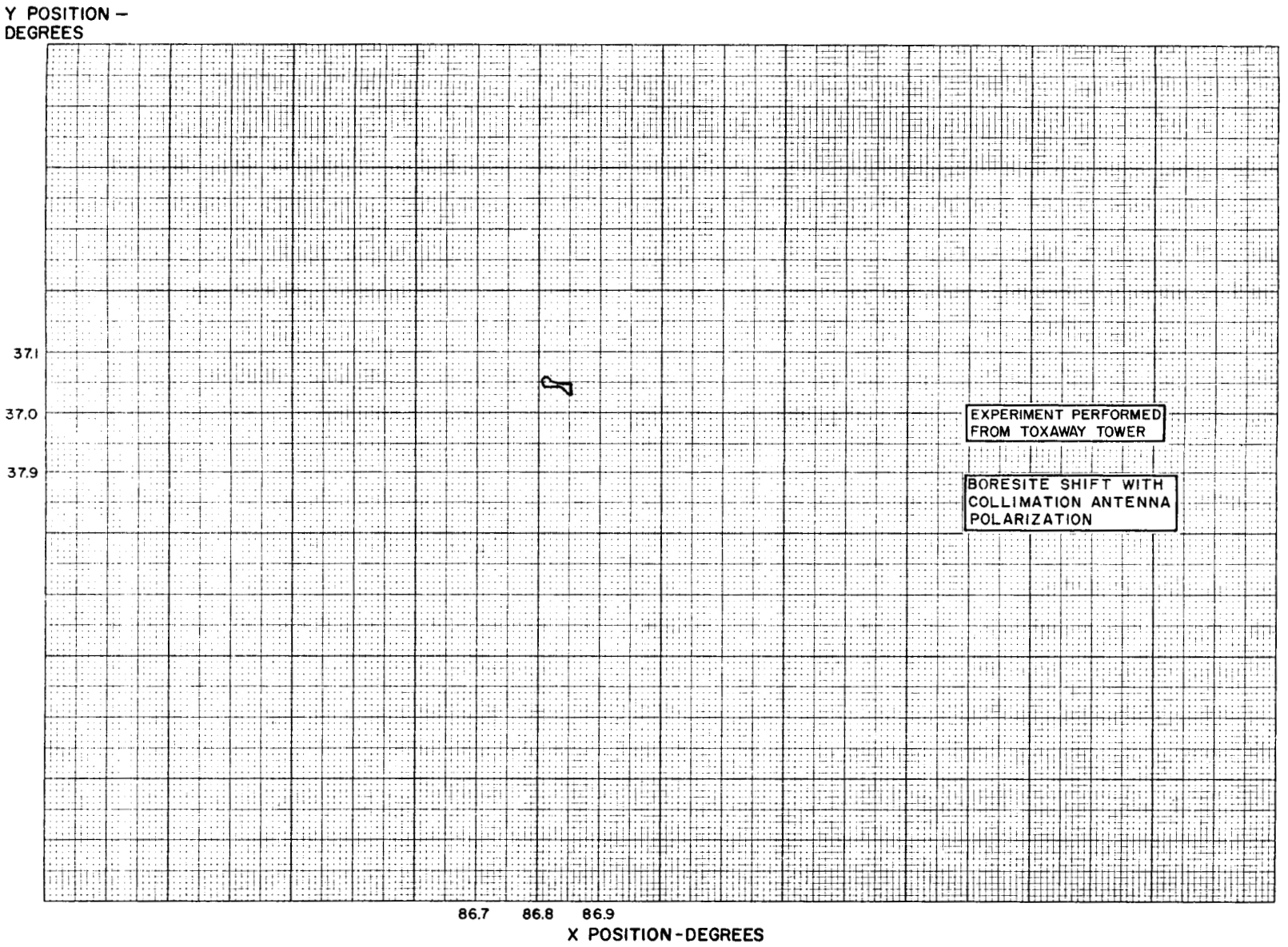

Figure 2-22. R-F Boresight Shift, RHC Polarization, 1700 Mc

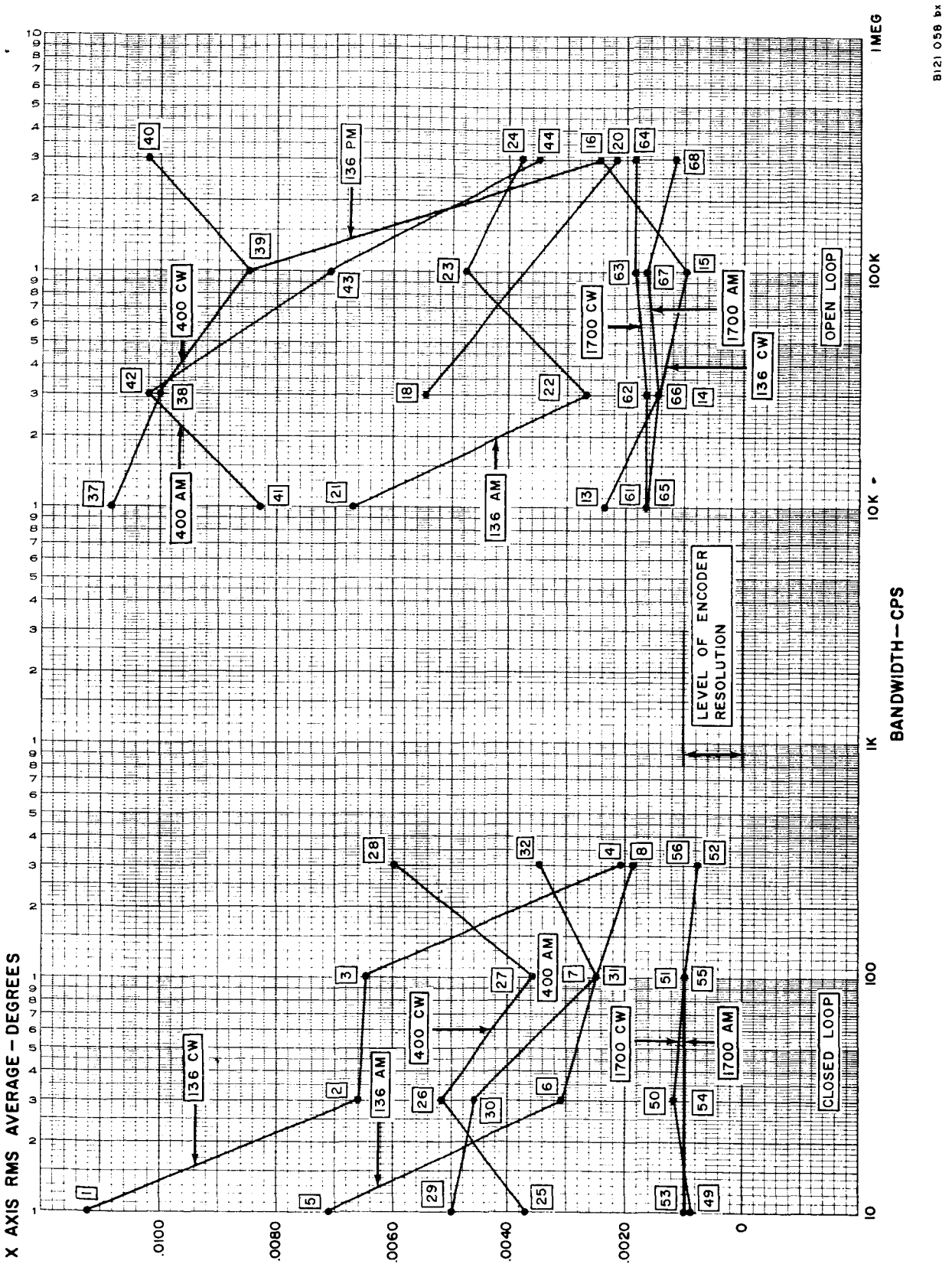

Figure 2-23. Static Tracking Stability, X-Axis RMS Average Versus Bandwidth

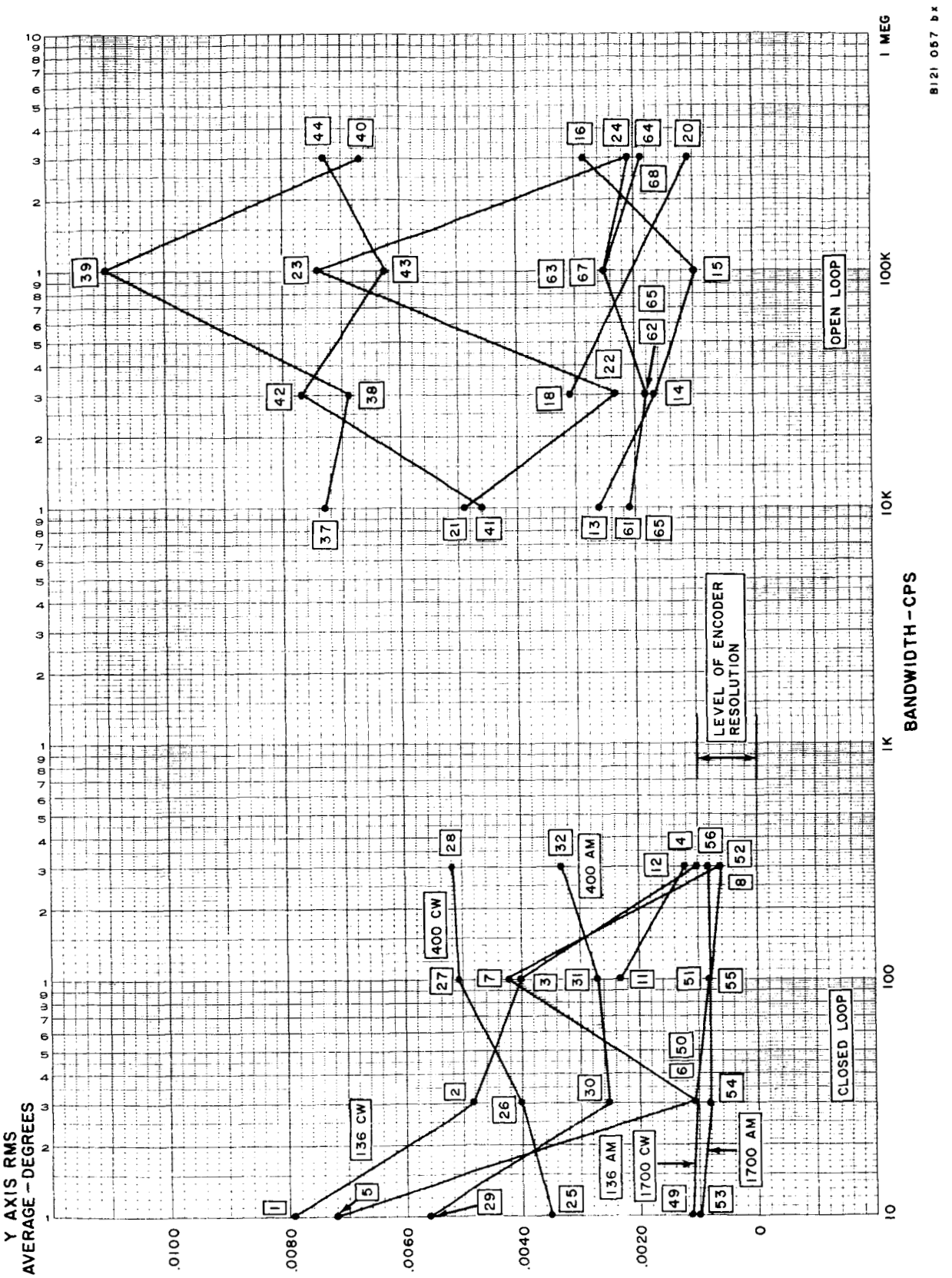

Figure 2-24. Static Tracking Stability, Y-Axis RMS Average Versus Bandwidth

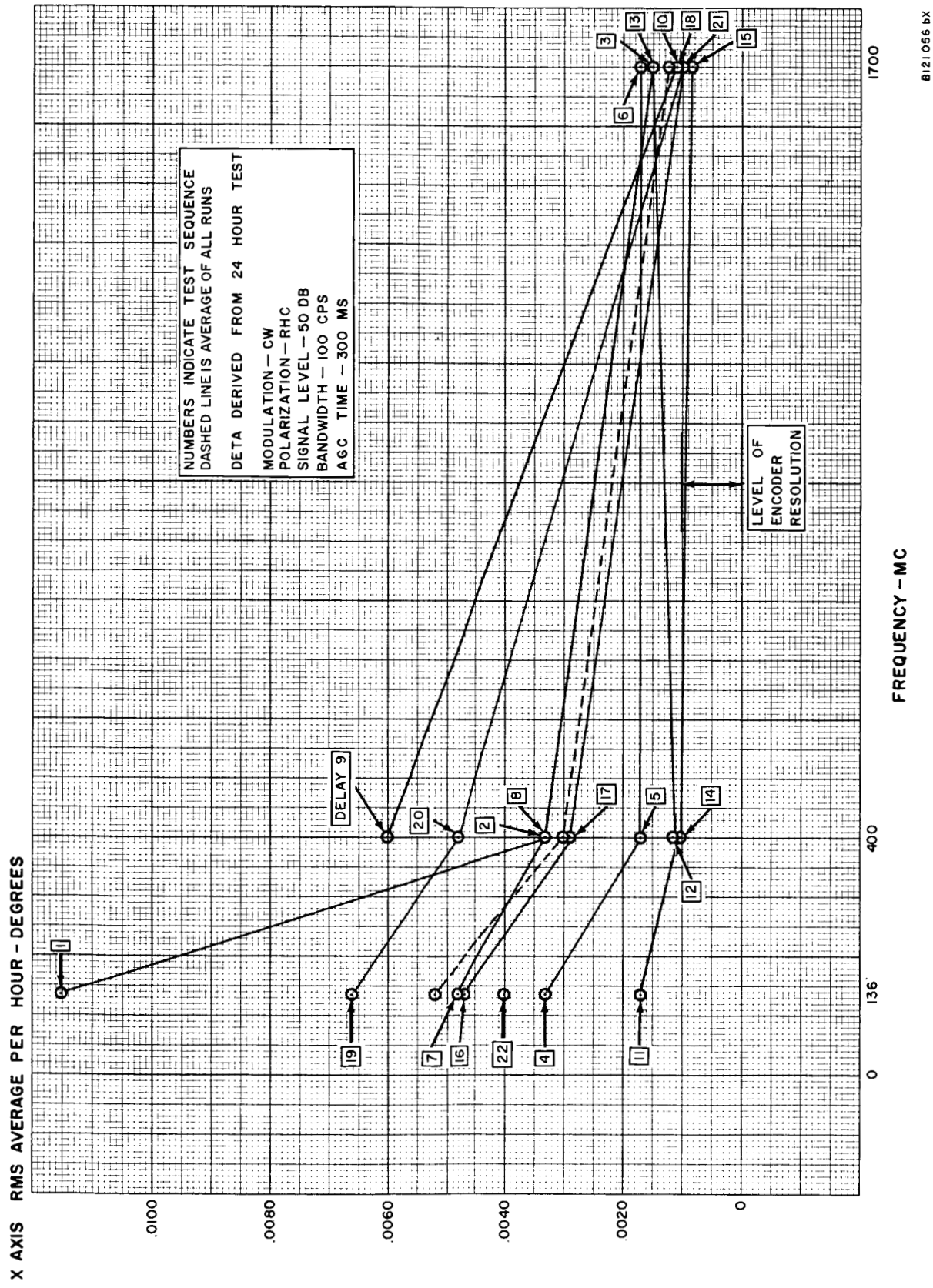

Figure 2-25. Static Tracking Stability, X-Axis RMS Average Versus Frequency

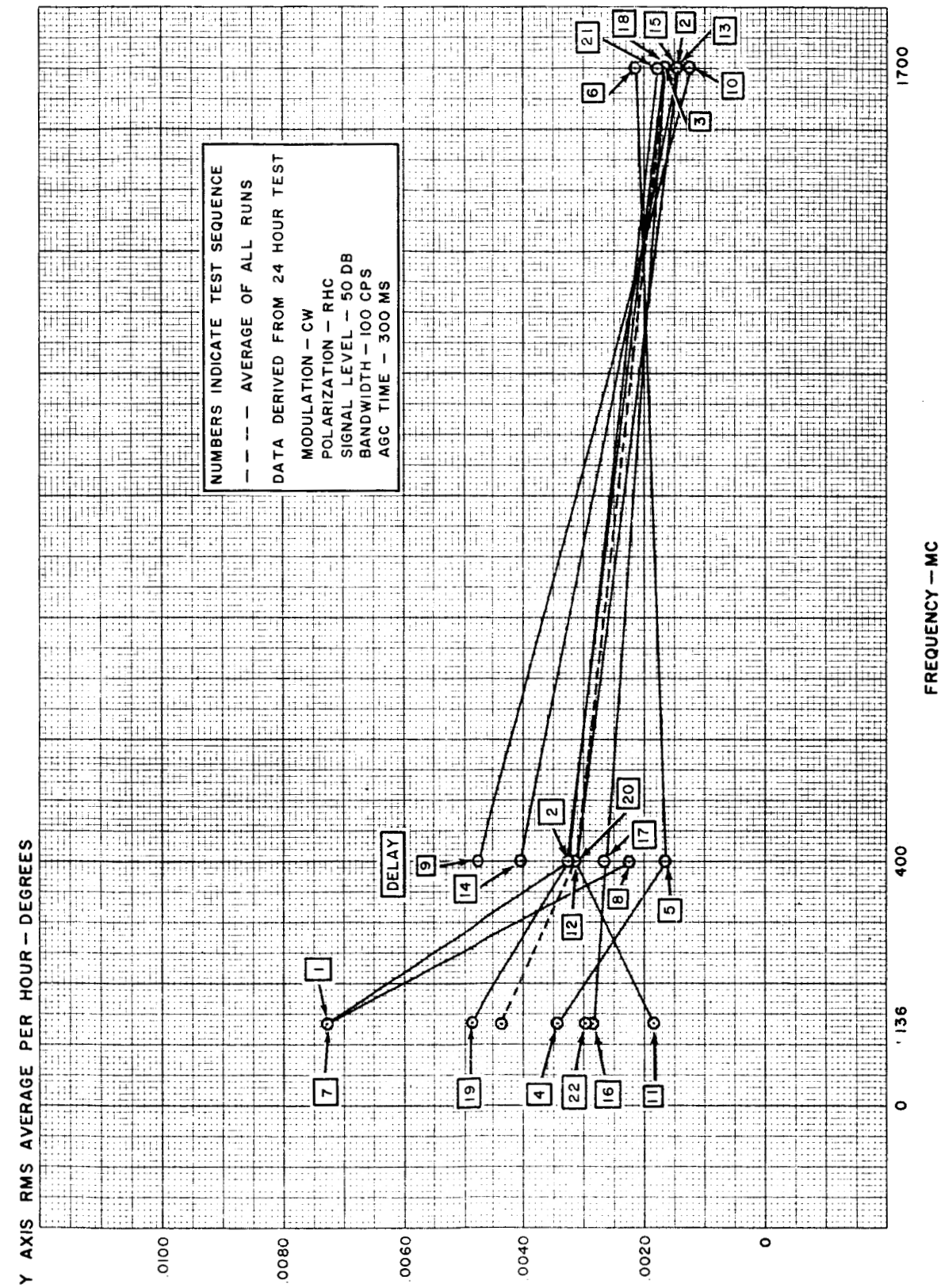

Figure 2-26. Static Tracking Stability, Y-Axis Average Versus Frequency

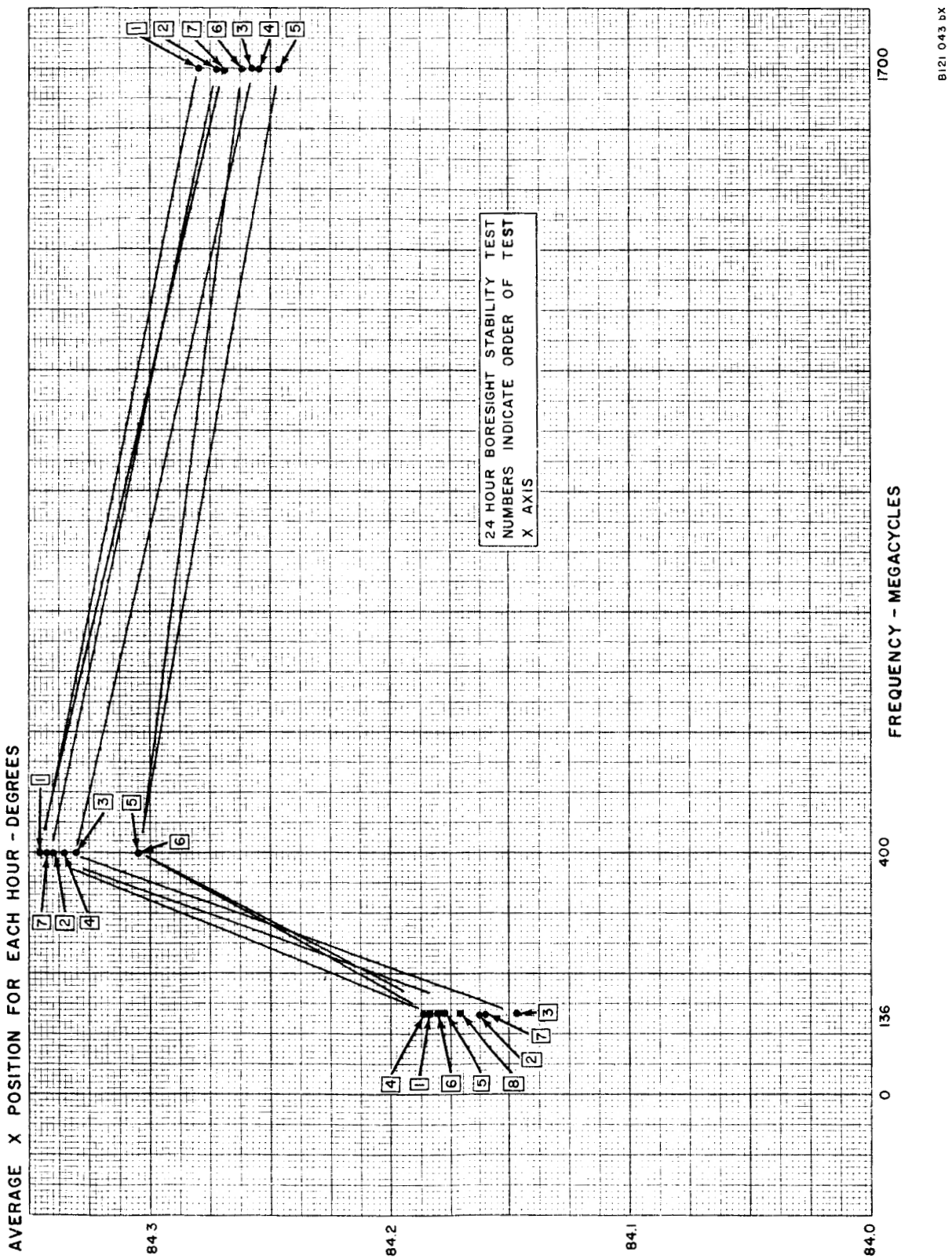

Figure 2-27. Static Tracking Stability, Average X Position for Each Hour

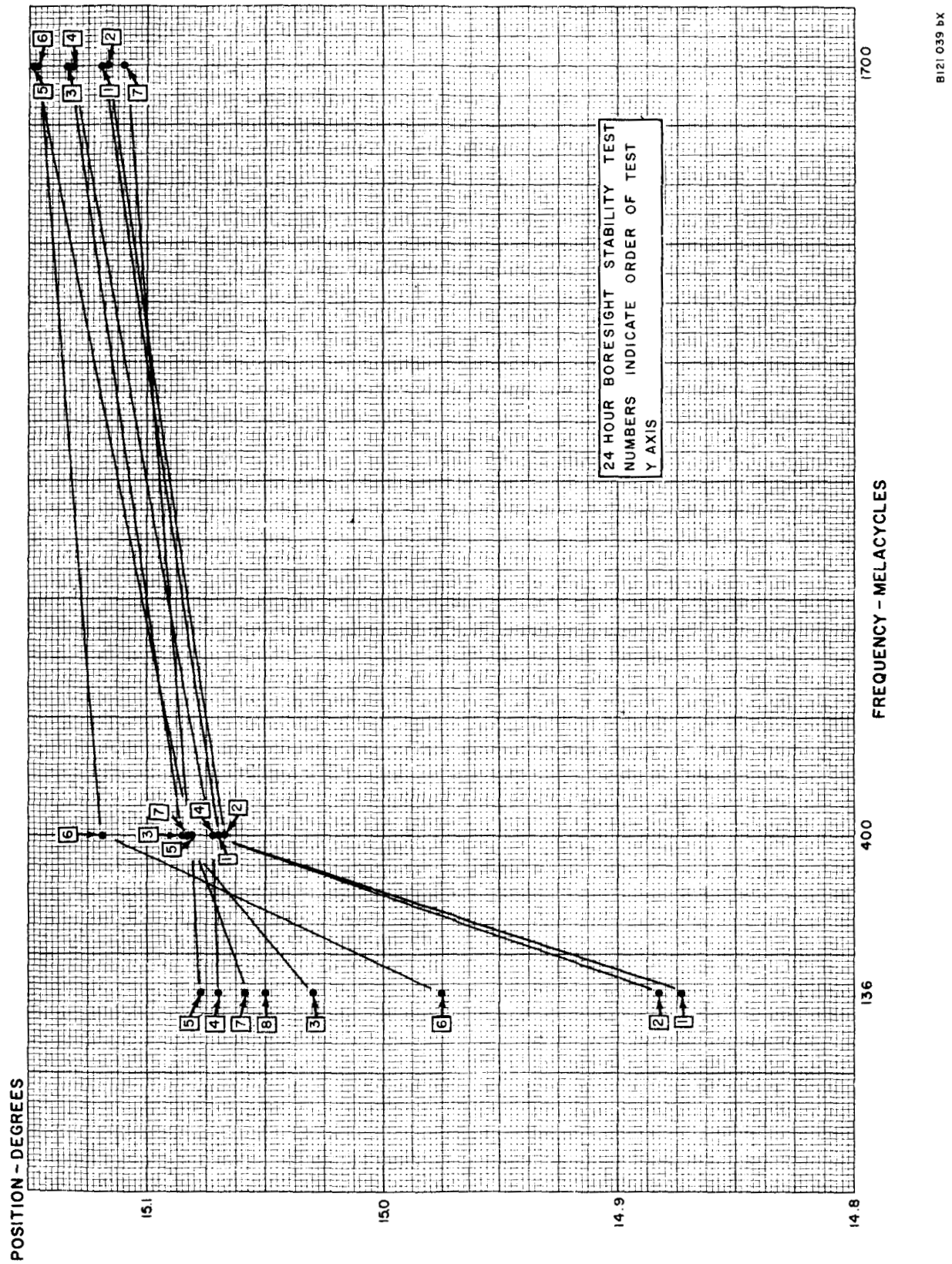

Figure 2-28. 24-Hour Boresight Stability Test, Y-Axis

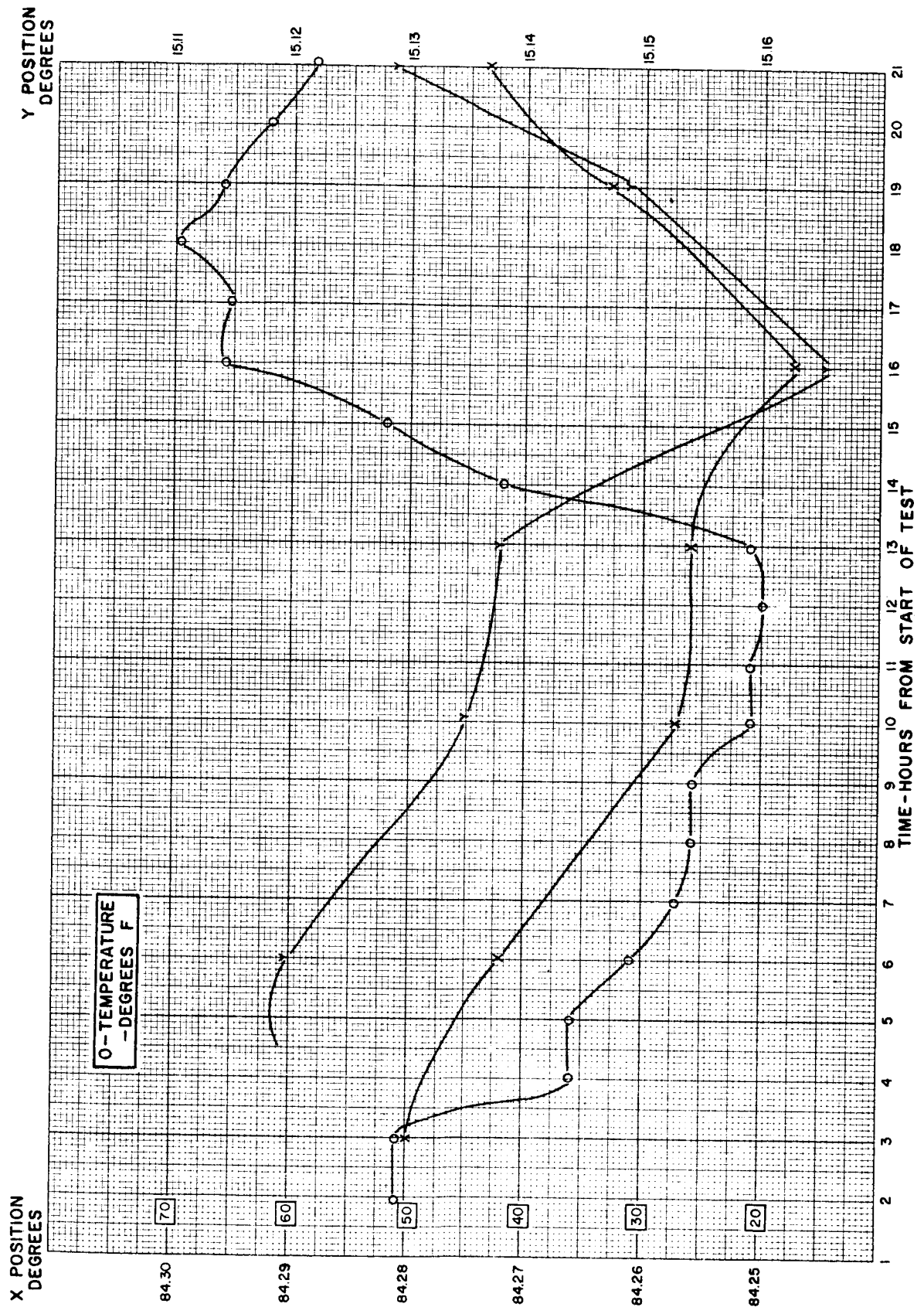

Figure 2-29. 24-Hour Boresight Stability Test, Position and Temperature (1700 Mc)

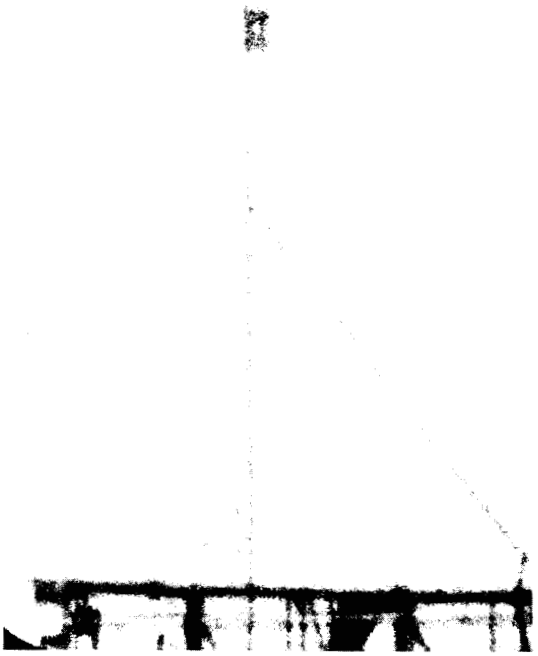

Note that the arm extends from the r-f source on the collimation tower by a distance equal to the displacement between the r-f and optical source on the antenna.

Note that aircraft at 10, 500 feet altitude and two lights are 18 inches apart on aircraft and displaced from r-f target by 12. 64 feet. The offset includes a velocity component of 0. 5°/sec in Y and 2. 2°/sec in X.

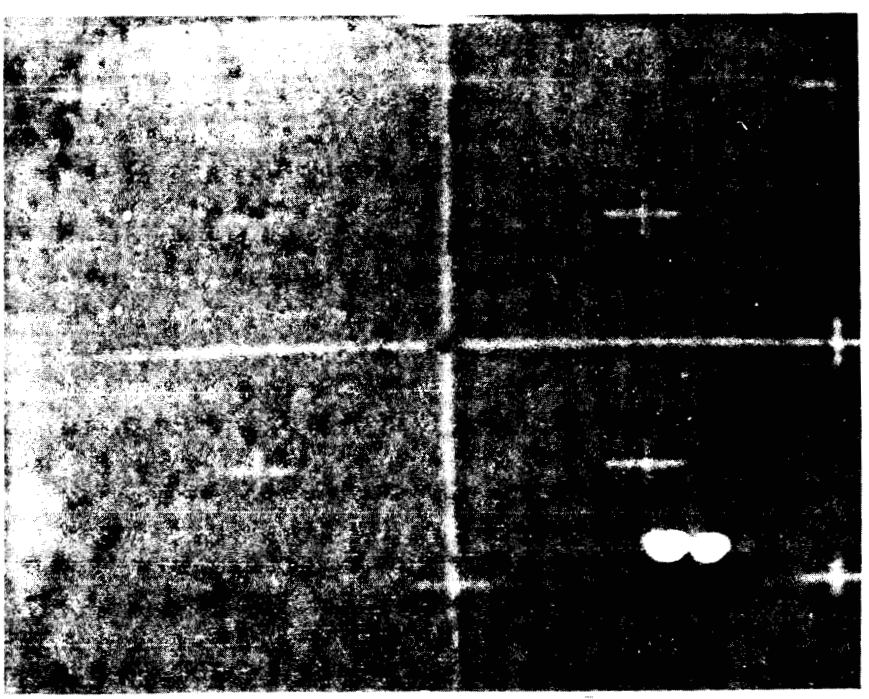

Figure 2-30. Typical Optical Boresight and Aircraft Track Frames

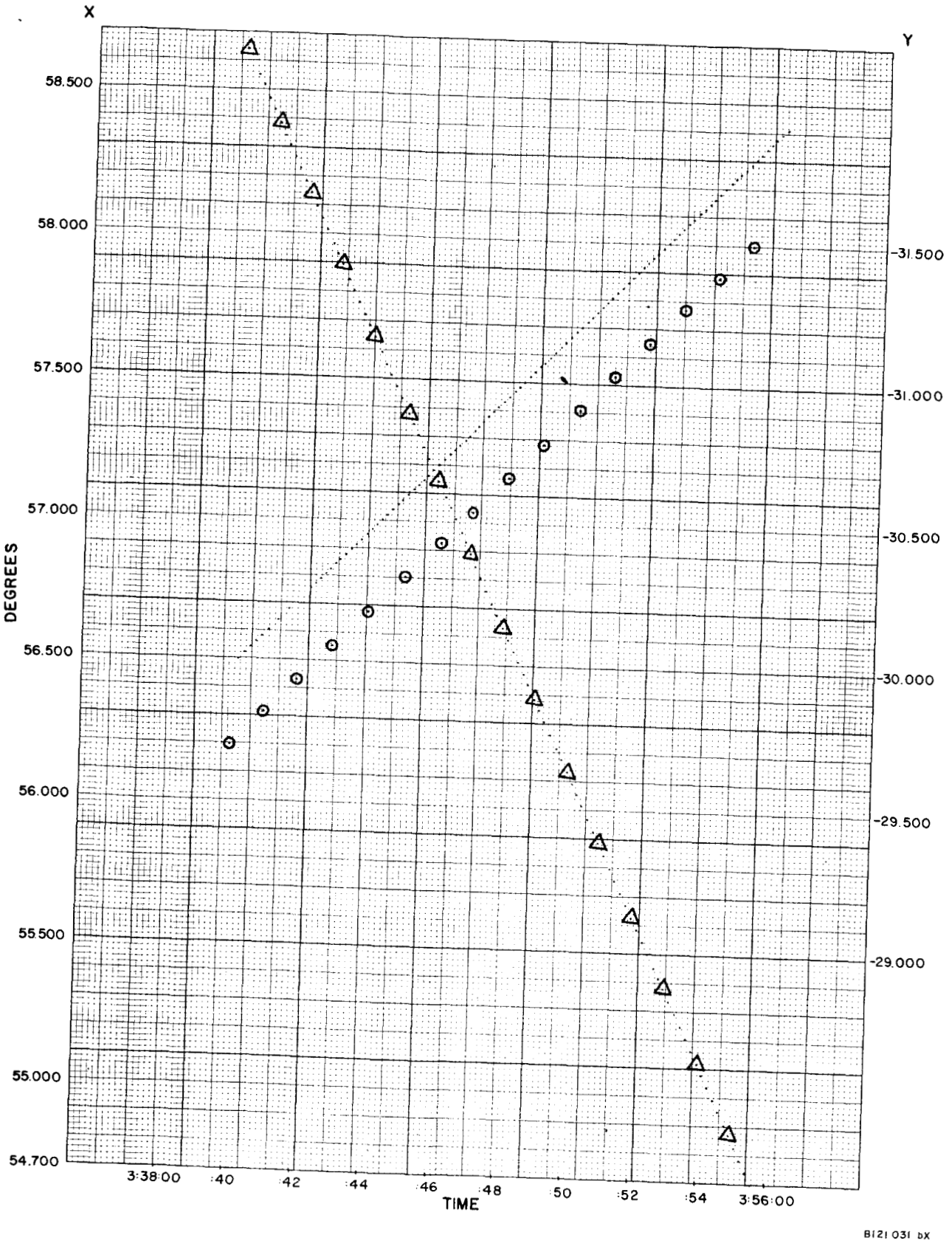

Figure 2-31. Program Star Track, Rigel

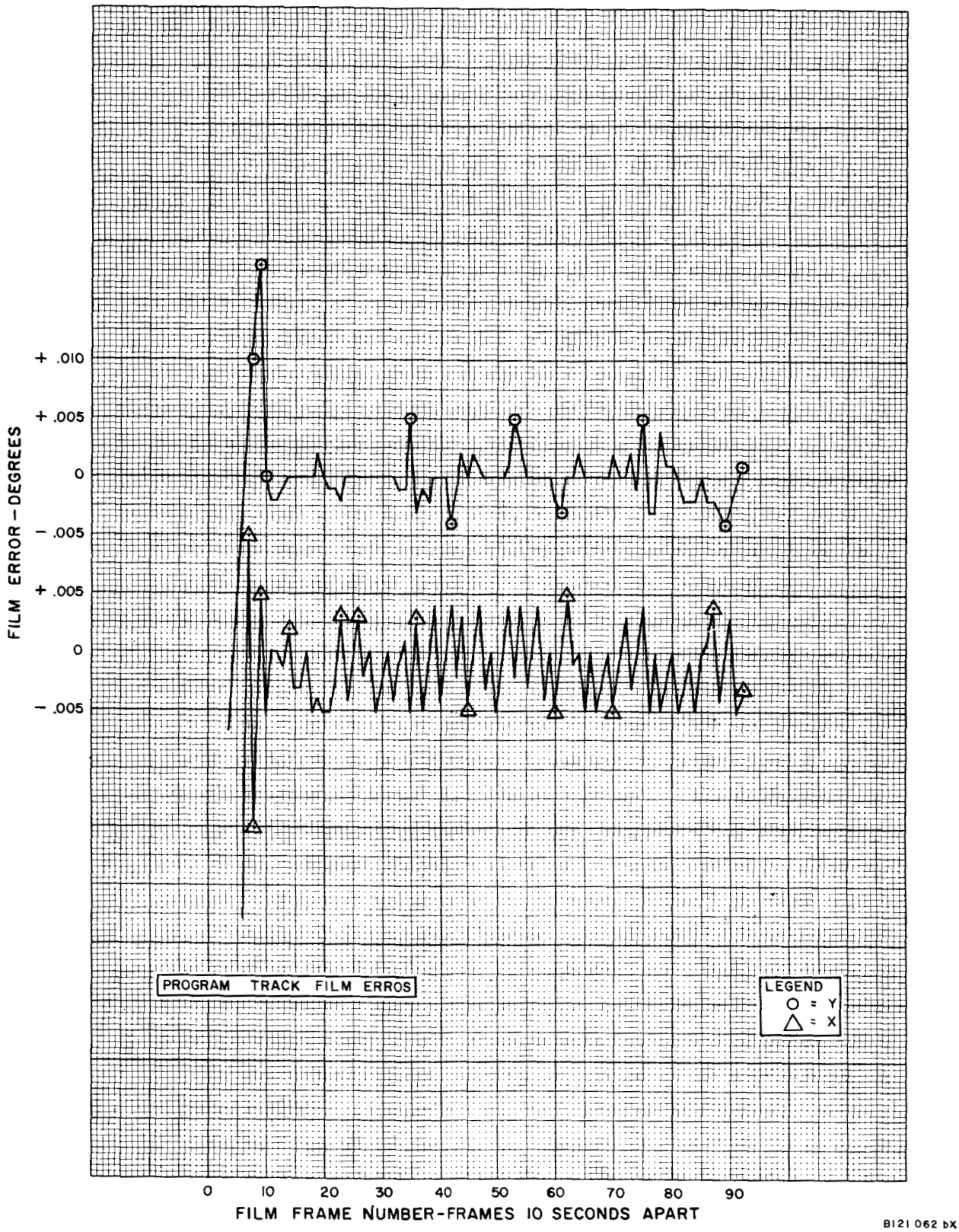

Figure 2-32. Program Track Film Errors

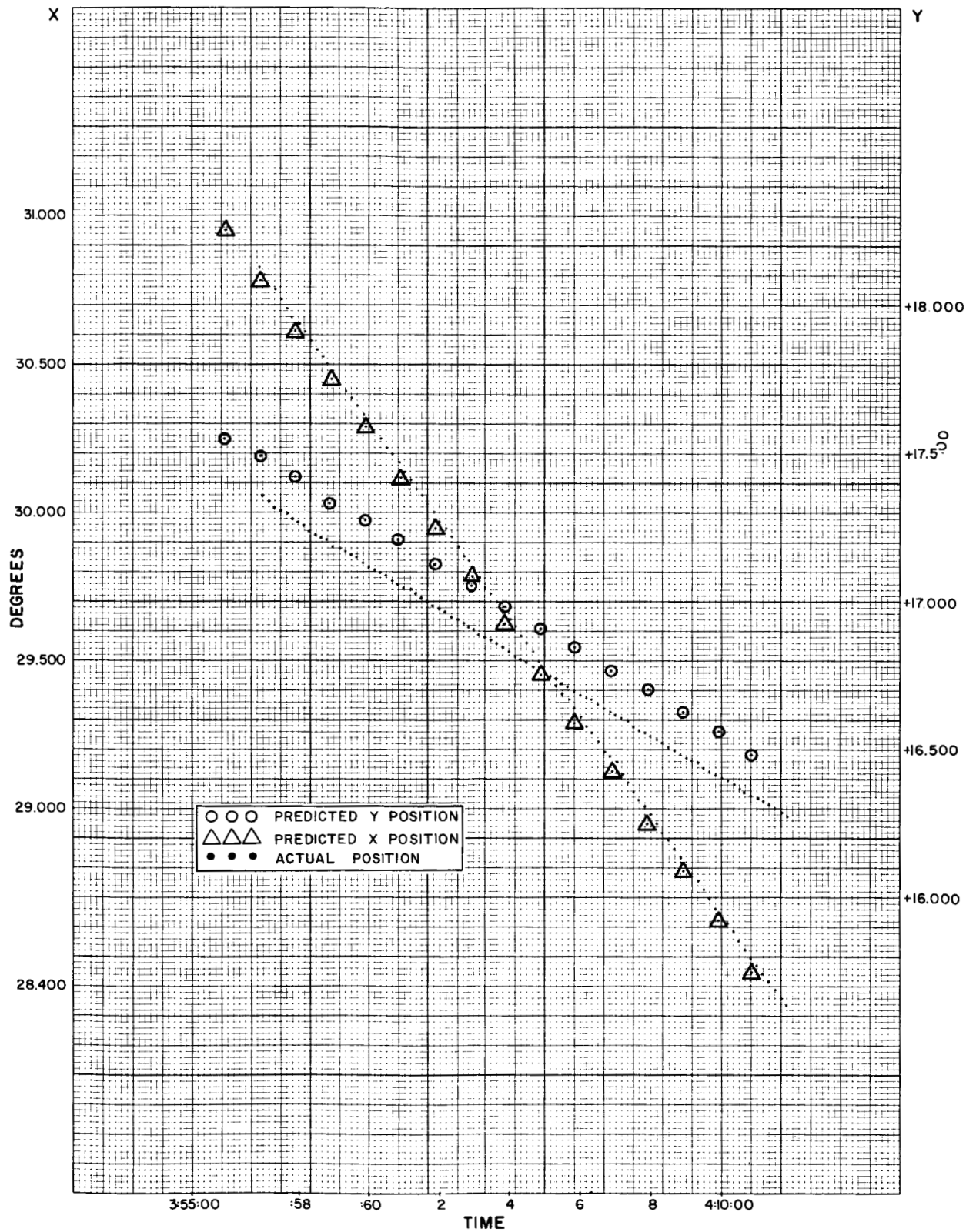

Figure 2-33. Program Star Track, Capella

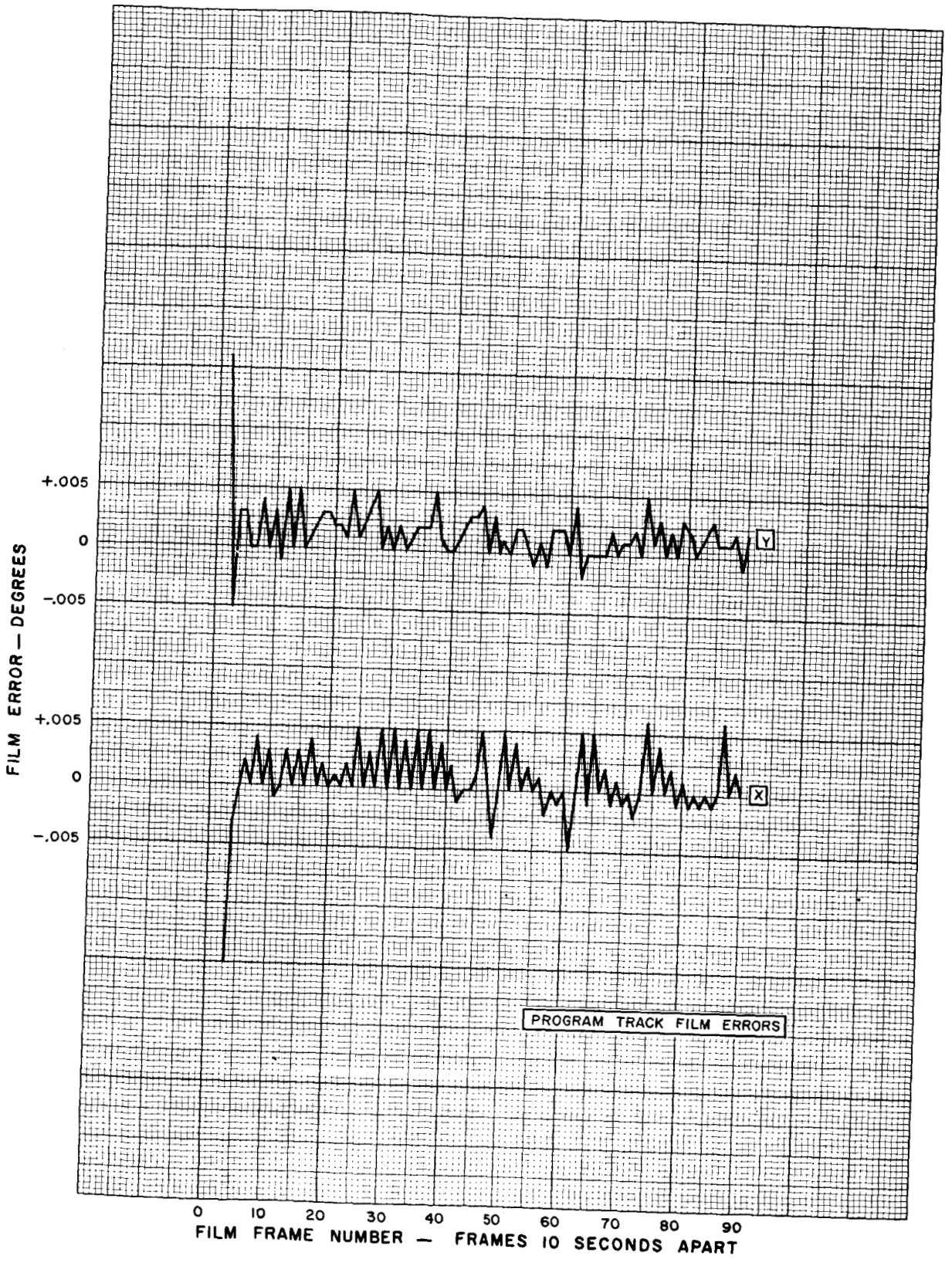

Figure 2-34. Program Track Film Errors Capella

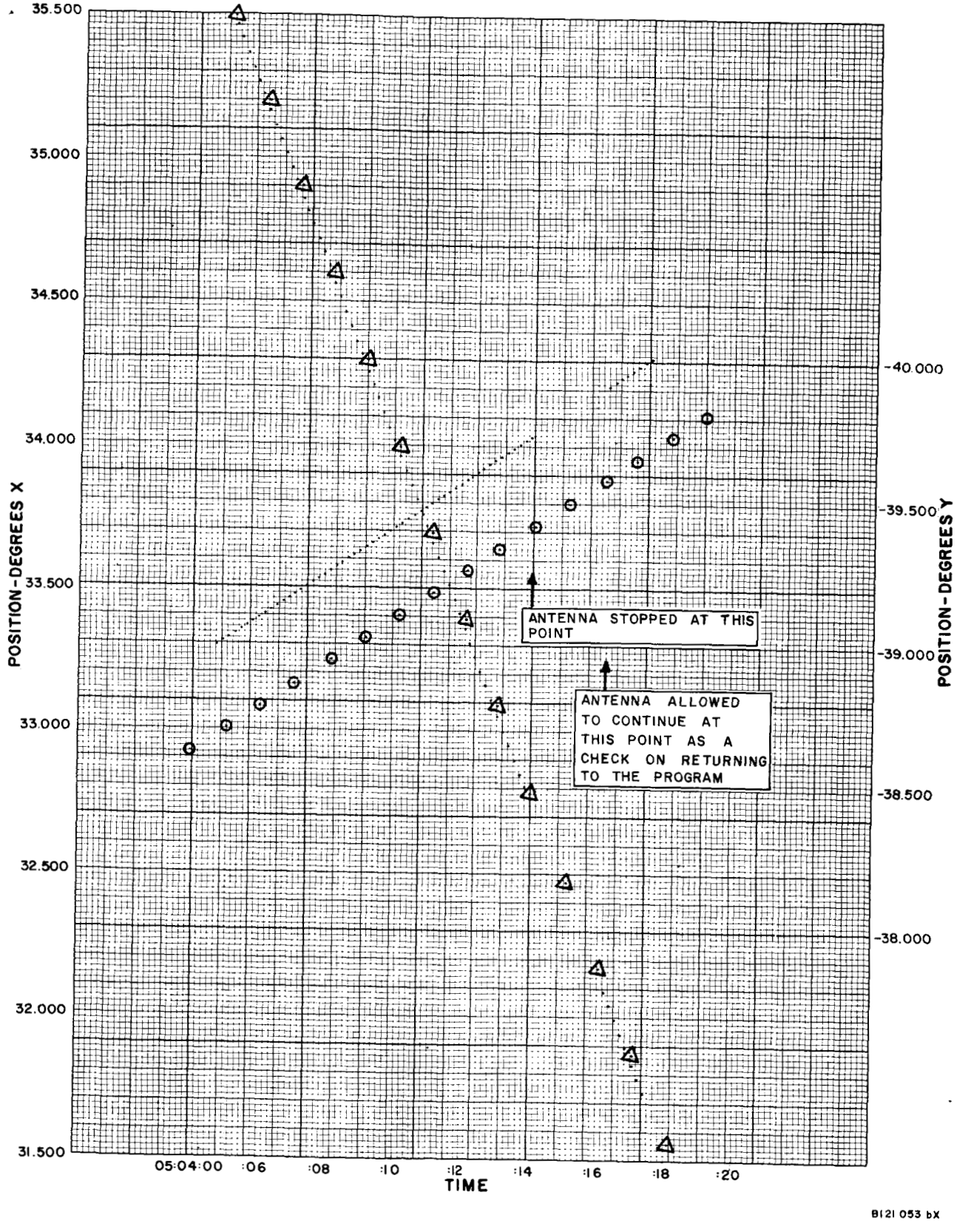

Figure 2-35. Program Star Track, Rigel

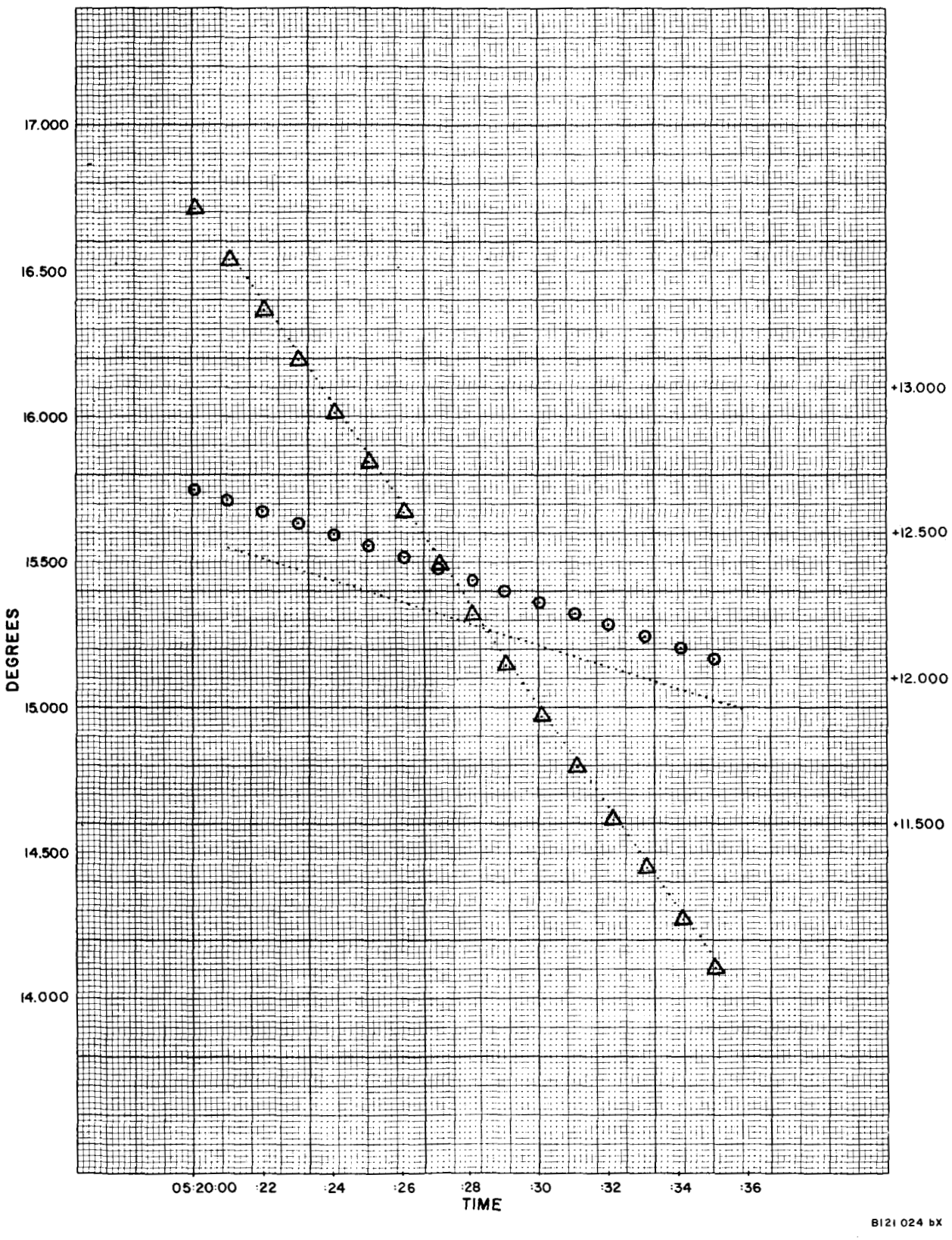

Figure 2-36. Program Star Track, Capella

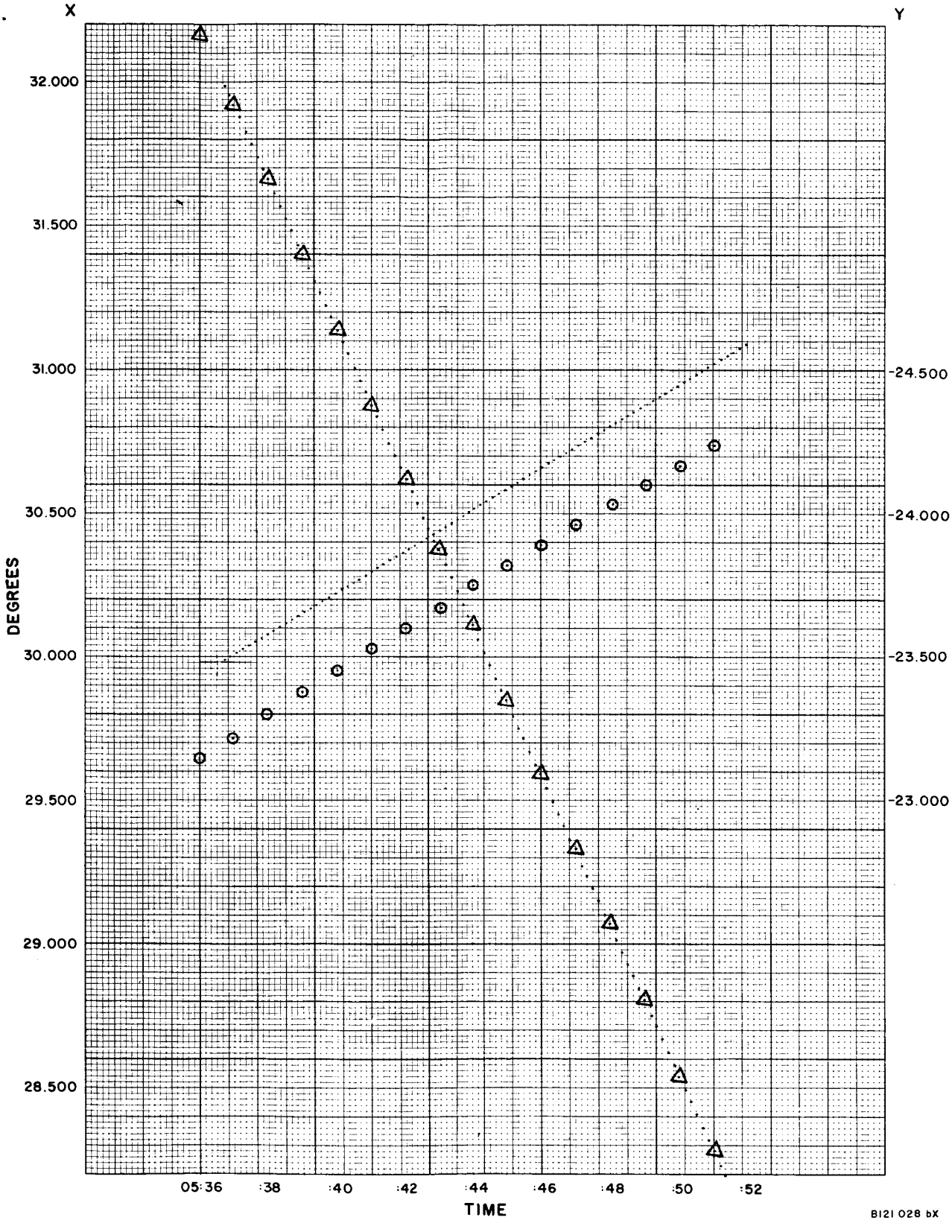

Figure 2-37. Program Star Track, Betelguese

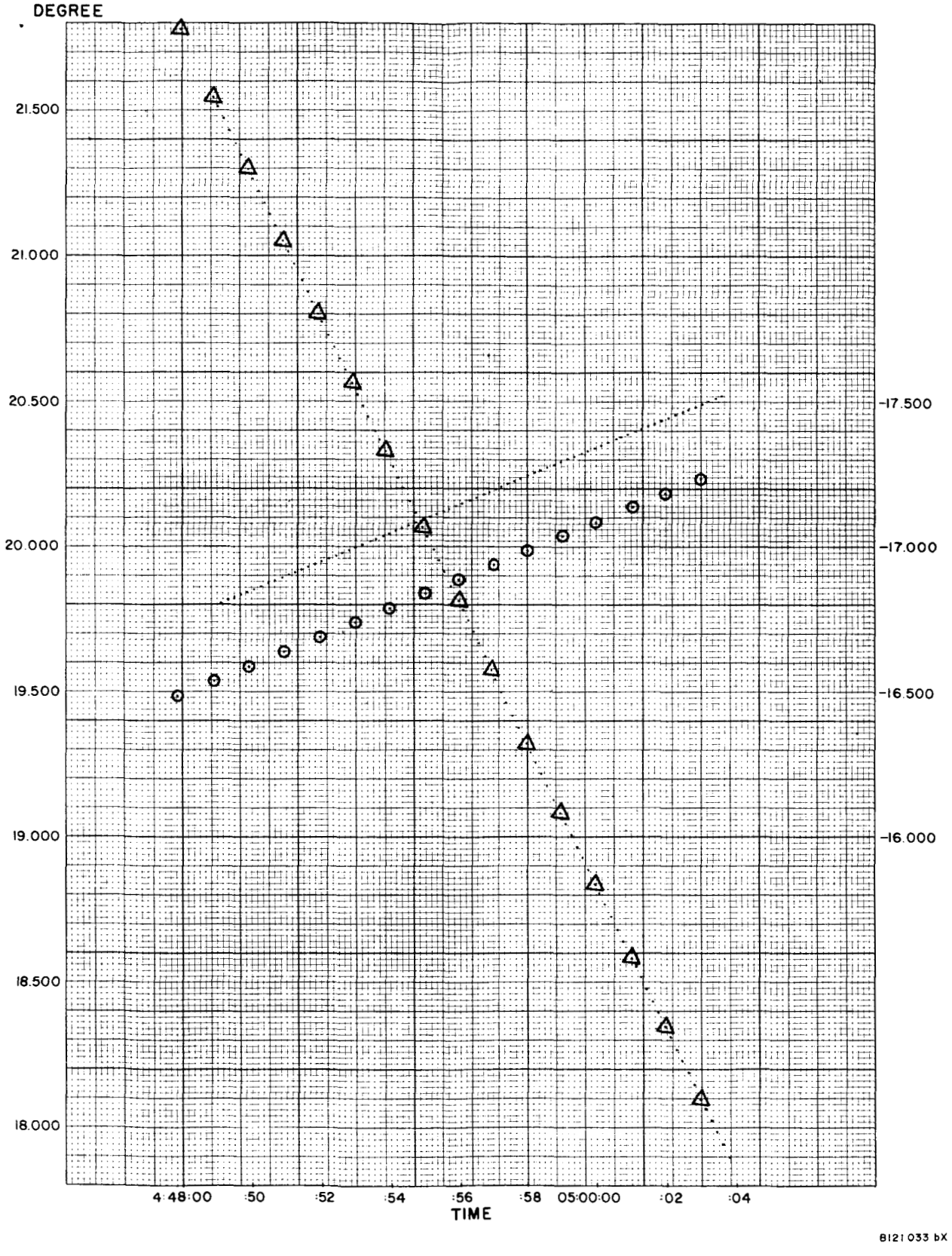

Figure 2-38. Program Star Track, Aldebaran

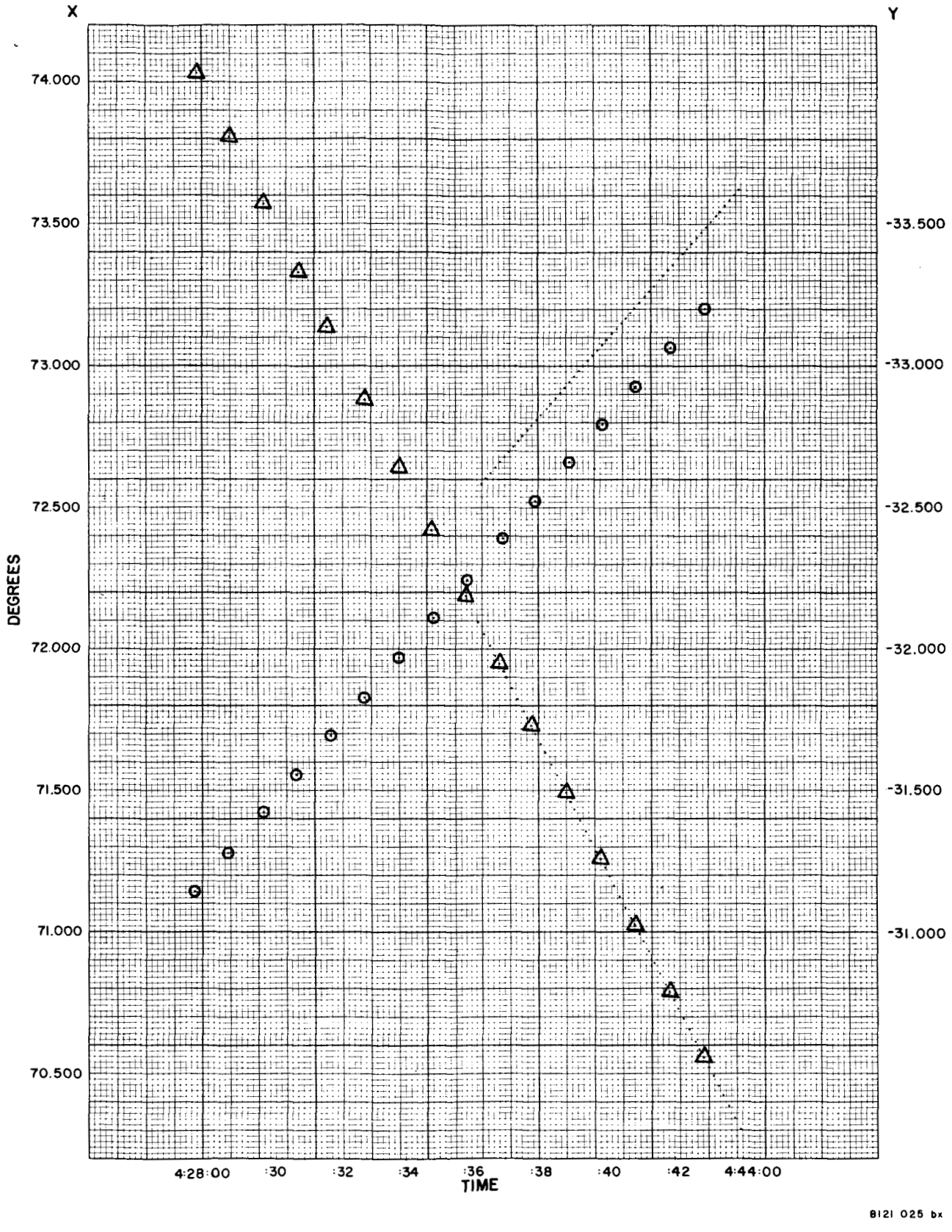

Figure 2-39. Program Star Track, Sirius

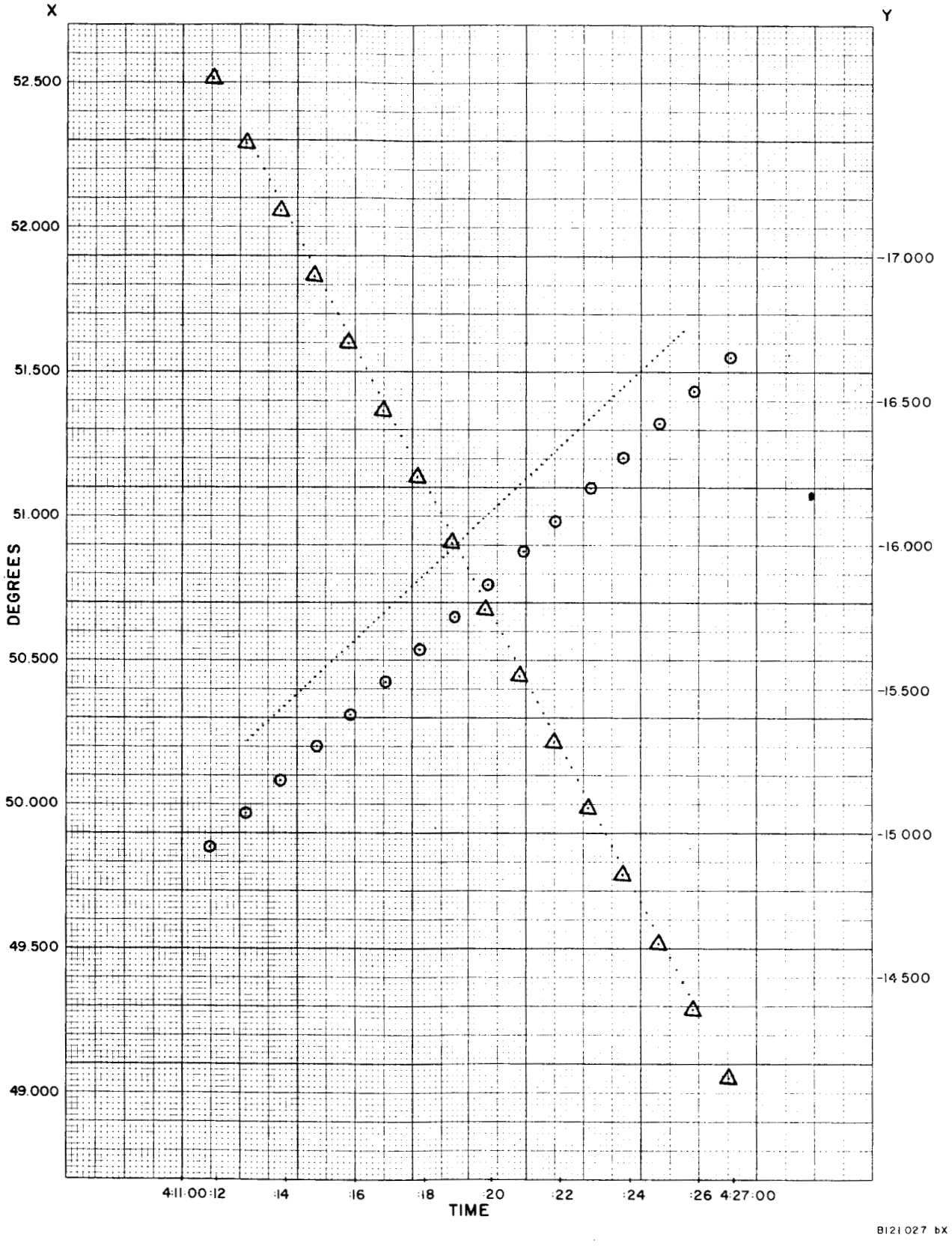

Figure 2-40. Program Star Track, Betelguese

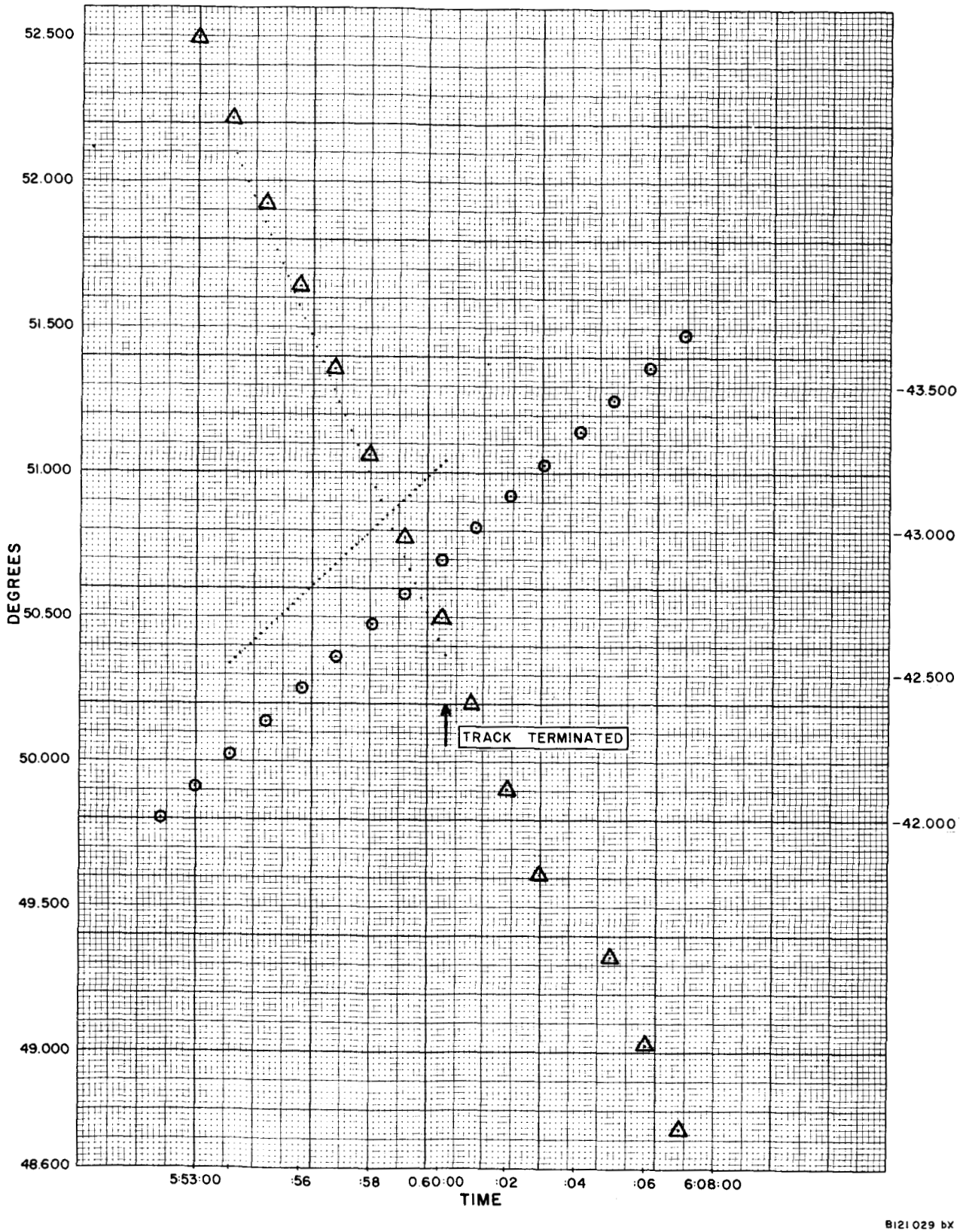

Figure 2-41. Program Star Track, Sirius